AD_____

Award Number: DAMD17-02-1-0492

TITLE: Suppression of NFkB by Tetrathiomolybdate Inhibits Tumor Angiogenesis and
Enhances Apoptosis in Human Breast Cancers

PRINCIPAL INVESTIGATOR: Quintin Pan, Ph.D.

CONTRACTING ORGANIZATION: The University of Michigan
Ann Arbor, MI 48109-1274

REPORT DATE: May 2005

TYPE OF REPORT: Annual Summary

20060309 108

PREPARED FOR: U.S. Army Medical Research and Materiel Command
Fort Detrick, Maryland 21702-5012

DISTRIBUTION STATEMENT: Approved for Public Release;
Distribution Unlimited

The views, opinions and/or findings contained in this report are those of the author(s) and
should not be construed as an official Department of the Army position, policy or decision
unless so designated by other documentation.

REPORT DOCUMENTATION PAGE

Form Approved
OMB No. 0704-0188

Public reporting burden for this collection of information is estimated to average 1 hour per response, including the time for reviewing instructions, searching existing data sources, gathering and maintaining the data needed, and completing and reviewing this collection of information. Send comments regarding this burden estimate or any other aspect of this collection of information, including suggestions for reducing this burden to Department of Defense, Washington Headquarters Services, Directorate for Information Operations and Reports (0704-0188), 1215 Jefferson Davis Highway, Suite 1204, Arlington, VA 22202-4302. Respondents should be aware that notwithstanding any other provision of law, no person shall be subject to any penalty for failing to comply with a collection of information if it does not display a currently valid OMB control number. **PLEASE DO NOT RETURN YOUR FORM TO THE ABOVE ADDRESS.**

1. REPORT DATE (DD-MM-YYYY)	2. REPORT TYPE	3. DATES COVERED (From - To)
01-05-2005	Annual Summary	1 May 2002 - 30 Apr 2005

4. TITLE AND SUBTITLE	5a. CONTRACT NUMBER
Suppression of NFkB by Tetrathiomolybdate Inhibits Tumor Angiogenesis and Enhances Apoptosis in Human Breast Cancers	
	5b. GRANT NUMBER
	DAMD17-02-1-0492
	5c. PROGRAM ELEMENT NUMBER

6. AUTHOR(S)	5d. PROJECT NUMBER
Quintin Pan, Ph.D.	
	5e. TASK NUMBER
	5f. WORK UNIT NUMBER
E-mail: qpan@med.umich.edu	

7. PERFORMING ORGANIZATION NAME(S) AND ADDRESS(ES)	8. PERFORMING ORGANIZATION REPORT NUMBER
The University of Michigan Ann Arbor, MI 48109-1274	

9. SPONSORING / MONITORING AGENCY NAME(S) AND ADDRESS(ES)	10. SPONSOR/MONITOR'S ACRONYM(S)
U.S. Army Medical Research and Materiel Command Fort Detrick, Maryland 21702-5012	
	11. SPONSOR/MONITOR'S REPORT NUMBER(S)

12. DISTRIBUTION / AVAILABILITY STATEMENT
Approved for Public Release; Distribution Unlimited

13. SUPPLEMENTARY NOTES

14. ABSTRACT
Angiogenesis, the formation of capillaries from pre-existing blood vessels, is essential for sustained growth of solid tumors. Numerous studies have shown that copper is required to modulate several pro-angiogenic factors. However, the specific effects of copper homeostasis on tumor angiogenesis have not been extensively studies. Our preliminary studies demonstrated that tetrathiomolybdate, a potent and novel copper chelator, blocks tumor growth and angiogenesis. We hypothesize that TM is inhibiting tumor angiogenesis by decreasing levels of VEGF, bFGF, IL-6, and IL-8 through interference with the NFkB signaling cascade. In this proposal, the molecular mechanism whereby TM regulates NFkB expression and activity will be investigated. We will establish if the NFkB transcription factor complexes, p50, p52, RelA, and RelB are regulated by TM using western blot analysis and gel shift assays. Furthermore, using a reporter gene system, we will ascertain if TM regulation of VEGF, bFGF, IL-6, and IL-8 is a direct consequence of NFkB signal inhibition. The studies as outlined will help us better understand the role of copper deficiency in tumor angiogenesis and may lead to a more specific and potent global anti-angiogenic approach to treat breast cancer.

15. SUBJECT TERMS
NFkappaB, tetrathiomolybdate, breast cancer

16. SECURITY CLASSIFICATION OF:			17. LIMITATION OF ABSTRACT	18. NUMBER OF PAGES	19a. NAME OF RESPONSIBLE PERSON USAMRMC
a. REPORT U	b. ABSTRACT U	c. THIS PAGE U	UU	27	19b. TELEPHONE NUMBER (include area code)

Standard Form 298 (Rev. 8-98)
Prescribed by ANSI Std. Z39.18

Table of Contents

Introduction:

The NFκB/Rel family of transcription factors is comprised of RelA, RelB, c-Rel, p50 (nfκb1), and p52 (nfκb2) (1). In recent years, evidence linking uncontrolled NFκB activity to oncogenesis has emerged. NFκB has been shown to regulate genes important for invasion, angiogenesis, and metastasis. These include pro-angiogenic factors, such as VEGF, IL-6, and IL-8, matrix metalloproteinases, urokinase plasminogen activator (uPA), and cell adhesion molecules, such as ICAM-1 and VCAM-1 (2-6). Blocking NFκB activity in human ovarian cancer cells was shown to inhibit VEGF and IL-8 expression resulting in a decrease in tumor angiogenesis (7). Using SUM149 human inflammatory breast cancer cells, we demonstrate that p50 (nfκb1) and RelA protein levels are decreased in response to TM. Our preliminary data indicate that TM also was able to block NFκB-dependent transcription in these cells. Moreover, apoptosis was increased 2-fold in SUM149 cells following TM treatment. Taken together, our data lead us to hypothesize that TM is blocking tumor angiogenesis by decreasing levels of pro-angiogenic mediators, VEGF, bFGF, IL-6, and IL-8, and inducing apoptosis through interference with the NFκB signaling cascade. The specific aims as outlined in this proposal will help us to better understand the role of copper deficiency in tumor angiogenesis and apoptosis and may lead to a more specific approach to treat breast and other cancers.

Body:

Task 1: To determine the molecular mechanism whereby TM regulates NFκB expression and activity in human breast cancers (Months 1-12).

We determined whether copper deficiency induced by TM is modulating NFκB-mediated signaling. SUM149 and non-tumorigenic immortalized human mammary epithelial (HME) cells were transiently transfected with pNFκB, a vector that contains four tandem copies of the κB consensus sequence upstream of the luciferase reporter gene. Endogenous NFκB activity was shown to be 2.5-fold higher in SUM149 cells in comparison to HME cells. This is
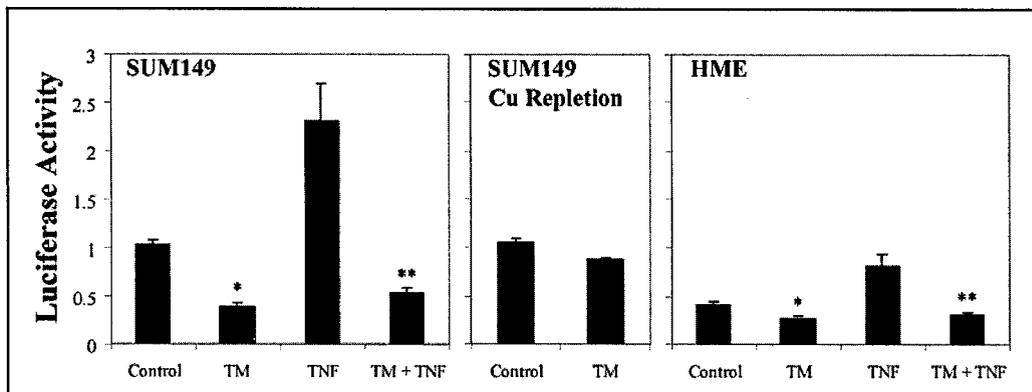

Figure 1. TM Suppresses NFκB-dependent Transcription. SUM149 or HME cells were transfected with pNFκB (Clontech Laboratories Inc.), a vector that contains four tandem copies of the κB consensus sequence fused to a TATA-like promoter region from the Herpes simplex virus thymidine kinase promoter. pRL-TK (Promega Corp.), a *Renilla* luciferase vector, was co-transfected into the cells to normalize for transfection efficiency. After a 24 hour recovery period, transfected cells were incubated in fresh medium with or without the addition of 2 nM CuSO$_4$. Cell were subsequently treated with vehicle, TM (1 nM), TNFα (2 pM), or TM and TNFα for 24 hours. *$P<0.001$; $n=6$, vehicle vs. TM. **$P<0.001$; $n=6$, vehicle or TNFα vs. TM + TNFα.

consistent with our observation that p50 protein levels were significantly higher in SUM149 cells (data not shown). After treatment for 24 hours, TM inhibited luciferase activity by 62±2% ($P<0.001$, $n=6$) in SUM149 cells and 34±2% ($P<0.001$, $n=3$) in HME cells (Figure 1). Moreover, TM completely blocked TNFα-stimulated NFκB activity in both cell lines. Similar results were observed at 48 and 72 hours demonstrating that TM is also able to inhibit NFκB activity on a sustained basis without affecting cell survival under these conditions. As shown in Figure 2, we analyzed the binding of nuclear proteins from SUM149 cells to a labeled oligonucleotide spanning the κB

4

consensus sequence. Extracts from TM-treated cells showed a decrease in nuclear protein binding to the κB consensus sequence. In addition, supershift analysis revealed that the predominant NFκB components in SUM149 cells are p50, p52, and RelA. When cells were cultured with added copper (2 nM CuSO₄ addition), TM partially lost its ability to regulate κB binding and NFκB transcriptional activity. Also, copper repletion partially reversed TM-inhibition of IL-6 and IL-8 mRNA expression, consistent with restoring NFκB's ability to enhance transcription of these genes. Interestingly, p50 and RelA protein levels were reduced following treatment with TM in SUM149 cells suggesting that TM may be suppressing NFκB activity by decreasing levels of NFκB component proteins.
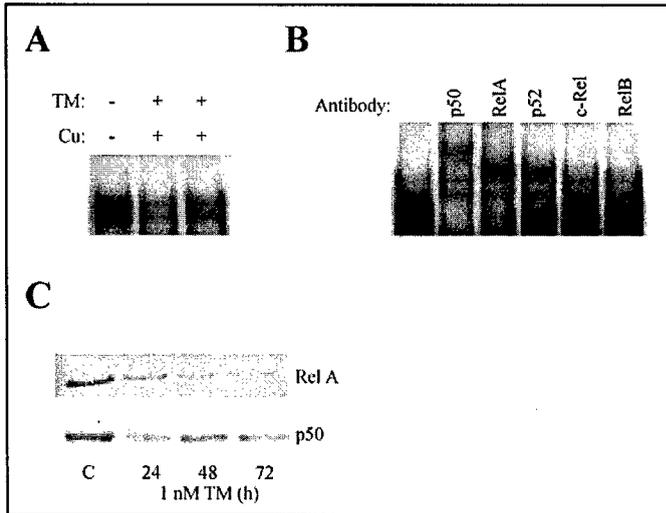

Figure 2. TM Decreases NFκB Binding and Protein Levels. **A,** Gel Shift Analysis. SUM149 cells were treated with vehicle or TM (1 nM) with or without the addition of 2nM CuSO₄ for 72 hours. Nucelar proteins were extracted, incubated with ³²P-labeled κB consensus sequence, and resolved by EMSA. **B,** Identification of NFκB Binding Complex. Supershift analysis was performed by pre-incubating nuclear extracts with p50, RelA, p52, c-Rel, or RelB antibody (Upstate Biotechnology) for 20 minutes on ice. **C,** p50 and RelA Protein Levels. SUM149 cells were treated with vehicle or TM (1 nM) for 72 hours. p50 and RelA levels were determined by Western blot analysis. Data is representative of three independent experiments.

Task 2: To determine if TM regulation of VEGF, bFGF, IL-6, and IL-8 is a direct consequence of inhibiting NFκB activity (Months 13-30).
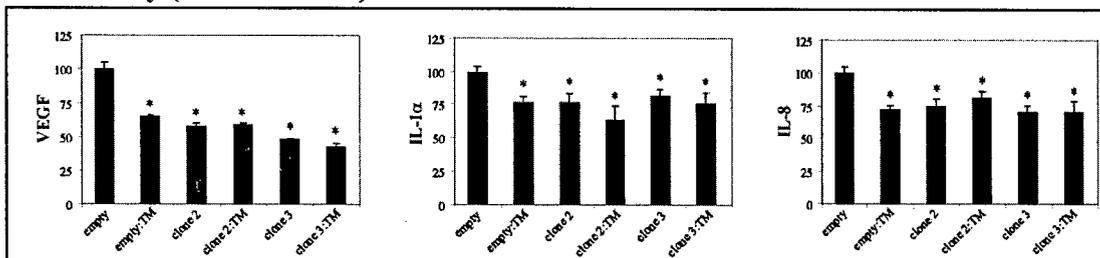

Figure 3. Characterization of proangiogenic mediators in SUM149 and SUM149-IκBαMut clones. SUM149, SUM149-empty, SUM149-IκBαMut clone2, or SUM149-IκBαMut clone3 cells were plated and treated with vehicle or 10 nM TM for 72 hours. Conditioned-media was collected and measured for VEGF, IL-1α and IL-8 by ELISA. *, p<0.05 vs. untreated SUM149-empty vector.

We characterized the effect of NFκB suppression in SUM149 cells by genetically inhibiting NFκB with a dominant negative IκBα (S32AS36A). As shown in Figure 3, conditioned-media from SUM149 wildtype and SUM149-IκBαMut clones were collected and measured for VEGF, IL-1α, and IL-8 by ELISA. Secretion of these proangiogenic mediators by SUM149 wildtype cells cells was significantly inhibited following TM treatment (10 nM for 72 hours). Similarly, SUM149-IκBαMut clones 2 and 3 secreted lower amounts of these proangiogenic mediators in comparison to untransfected or empty-vector transfected SUM149 cells (p<0.05) (Figure 2A). TM treatment of SUM149-

5

IκBαMut clones resulted in no additional effect on inhibiting the amount of proangiogenic mediators. Since the change in phenotype observed for TM-treated SUM149 cells are similar to untreated SUM149-IκBαMut clones and TM did not change the phenotype of SUM149-IκBαMut clones, there is evidence that inhibition of tumor angiogenesis by TM is a direct consequence of TM's ability to suppress NFκB activation.

Task 3: To determine if TM is inducing apoptosis through inhibition of NFκB activity in human breast cancers (Months 24-36):

Apoptosis was determined by flow cytometry using FITC-Annexin V. As shown in Figure 4A, cells treated with 1 nM TM resulted in 3.6 ± 1.1% of apoptotic cells. A concentration-dependent induction of apoptosis was observed with doxorubicin ranging from 9.9 ± 2.9% for 0.1 μM to 16.3 ± 2.1% for 0.5 μM. Doxorubicin (0.1 μM for 72 hours) induced 75 ± 3.4% apoptosis in MDA-MB435 and 60 ± 2.1% apoptosis in MDA-MB231. This observation indicates that SUM149 cells are relatively resistant to doxorubicin-induced apoptosis when compared to other commonly used breast carcinoma cell lines. SUM149 cells treated with the combination therapy resulted in a significant, greater than additive, increase in apoptosis in comparison to either compound administered alone; 33.8 ± 4.6% or 57.5 ± 5.2% (p<0.01, n=3) apoptosis was observed in cells treated with TM and 0.1 μM doxorubicin or TM and 0.5 μM doxorubicin, respectively. To determine whether the increase in apoptosis observed in the combination therapy was due to enhanced initiation of the caspase cascade, processed caspase-7 and PARP were measured (Figure 4B). Treatment with TM or doxorubicin alone did not induce significant caspase-7 or PARP cleavage. In contrast, the combination of TM and doxorubicin resulted in an increase in processed caspase-7 and PARP. These observations support the notion that the enhanced apoptosis observed with the combination therapy is due to an enhancement of caspase-mediated apoptosis.

Figure 4. Combination therapy of TM and doxorubicin enhances apoptosis *in vitro*. A, Flow cyotometric analysis of apoptotsis. SUM149 cells (2.5 x 10^5) were treated with control, 1 nM TM, 0.1 μM doxorubicin, 0.5 μM doxorubicin, 1 nM TM and 0.1 μM doxorubicin, or 1 nM TM and 0.5 μM doxorubicin for 72 hours. Apoptosis was determined by the FITC-annexinV/PI assay. Data is presented as mean ± SEM. *p<0.01 vs. TM treatment, **p<0.005 vs. TM or doxorubicin treatment. B, Western blot analysis of processed caspase-7 and PARP. SUM149 cells (2.5 x 10^5) were treated with control (lane 1), 1 nM TM (lane 2), 0.1 μM doxorubicin (lane 3), or 1 nM TM and 0.1 μM doxorubicin (lane 4) for 24 hours. Total protein lysates were separated by SDS-PAGE and immunoblotted using specific antibodies to caspase-7, PARP, and β-actin. These results are representative of three independent experiments.

Combination therapy of TM and doxorubicin suppresses tumor growth and enhances apoptosis. Female athymic nude mice were transplanted with SUM149 cells (1 X 10^6) and palpable tumors were allowed to develop

without treatment. At 28 days post-implantation, mice with established tumors of approximately 0.5 cm^3 were randomly assigned to four protocols and treated with control (gavaged with water daily and intravenous injection with PBS weekly), TM (1.25 mg/day loading dose for three days followed by 0.7 mg/day maintenance dose for remainder of protocol) by oral gavage, doxorubicin (5 mg/kg/week) by intravenous injection, or co-treated with TM (1.25 mg/day loading dose for three days followed by 0.7 mg/day maintenance dose for remainder of protocol) and doxorubicin (5 mg/kg/week). Although the doubling time of control SUM149 tumors appears to be around 19 days, the experiment was terminated at 28 days post-treatment due to general health concerns as the size of the mammary tumors were bulky enough to impede mice from the control group from eating and drinking. Mice treated with TM as a single agent or in combination with doxorubicin were rendered copper deficient (ceruloplasmin levels <25 ± 5% of control) after 1 week of therapy and remained so for the rest of the protocol. As shown in Figure 5, therapy with TM or doxorubicin alone significantly inhibited tumor growth in comparison to control mice (p<0.05, n=6). More importantly, mice treated with the combination of TM and doxorubicin resulted in complete tumor stabilization without an apparent increase in toxicity as assessed by general health, weight, and behavior (p<0.008 compared to control; p<0.03 compared to TM or doxorubicin; n=6).

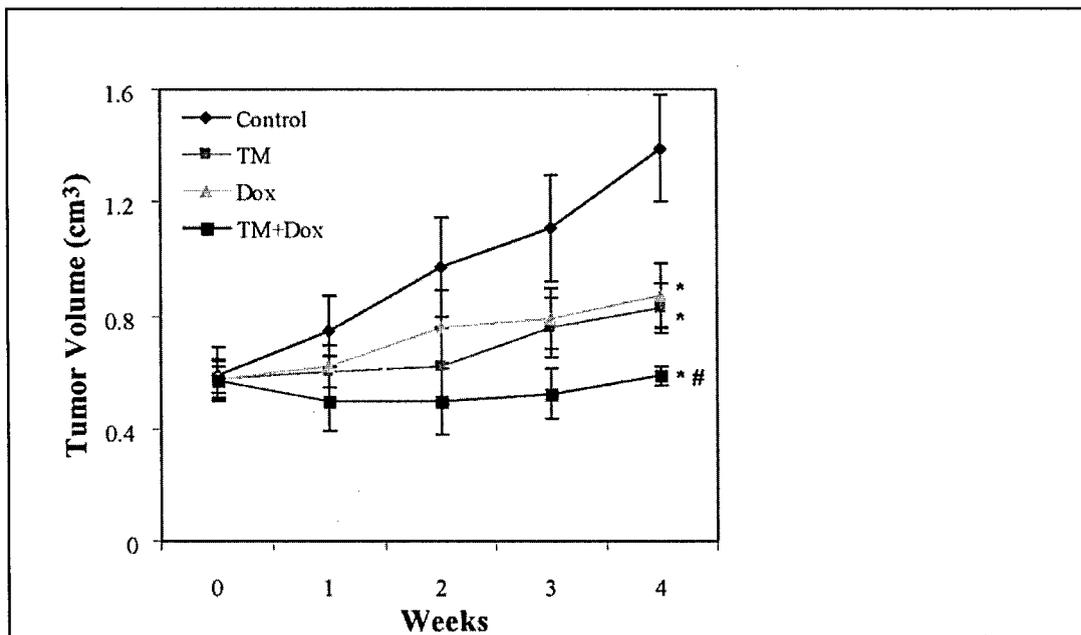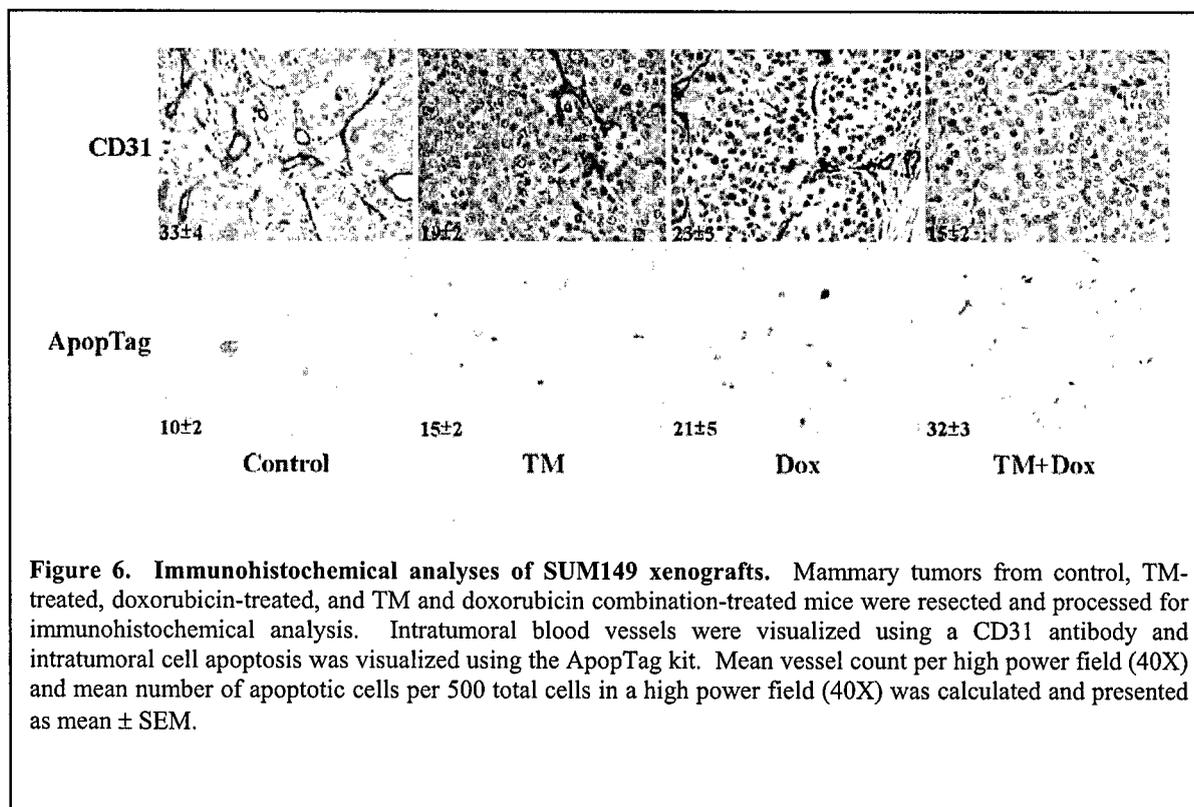**Figure 5. Combination therapy of TM and doxorubicin inhibits tumor growth in SUM149 xenografts.** SUM149 cells (1 X 10^6) were orthotopically injected in the upper left mammary fat pad of 10-week old athymic female mice. At 28 days post-implantation, mice with established tumors of approximately 0.5 cm^3 were randomly assigned to four protocols; control (gavaged with water daily and intravenous injection with PBS weekly), TM (1.25 mg/day loading dose for three days followed by 0.7 mg/day maintenance dose for remainder of protocol) by oral gavage, doxorubicin (5 mg/kg/week) by intravenous injection, or co-treated with TM (1.25 mg/day loading dose for three days followed by 0.7 mg/day maintenance dose for remainder of protocol) and doxorubicin (5 mg/kg/week). Tumor volume was calculated as (length X width^2)/2 and presented as mean ± SEM.. *p<0.05 vs. control group, #p<0.03 vs. TM- or doxorubicin-treated group; n=6 per treatment group.

Immunohistochemical analyses of the resected tumors revealed that intratumoral apoptosis was significantly higher than control in all treatment protocols (p<0.01); 50% increase in the TM-treated group, 110% increase in the doxorubicin-treated group, and 220% increase in the combination-treated group. Moreover, tumor cell apoptosis was significantly higher in the combination therapy group than in either single agent group of TM or doxorubicin (p<0.01). As expected, tumors from the control group were highly vascularized with a mean vessel count of 33 ± 4 (mean ± SEM) per high-power field. In contrast, the smaller tumors resected from TM- (19 ± 2, p<0.01), doxorubicin-

(23 ± 3, p<0.05), or TM and doxorubicin-treated (15 ± 2, p<0.01) mice were significantly less vascularized per high-power field. The difference in microvessel density between these three treatment groups did not reach statistical significance. Taken together, our data indicate that the combination therapy of TM and doxorubicin is more effective at suppressing tumor growth due to an increase in intratumoral apoptosis.

Figure 6. Immunohistochemical analyses of SUM149 xenografts. Mammary tumors from control, TM-treated, doxorubicin-treated, and TM and doxorubicin combination-treated mice were resected and processed for immunohistochemical analysis. Intratumoral blood vessels were visualized using a CD31 antibody and intratumoral cell apoptosis was visualized using the ApopTag kit. Mean vessel count per high power field (40X) and mean number of apoptotic cells per 500 total cells in a high power field (40X) was calculated and presented as mean ± SEM.

Key Research Accomplishments and Reportable Outcomes:

1. TM was found to significantly decrease NFκB protein levels and transcriptional activity.

2. TM was found to decrease the levels of potent proangiogenic mediators, VEGF, IL-1α, and IL-8.

3. We identified a major mechanism of the antiangiogenic effect of copper deficiency induced by TM is suppression of NFκB, contributing to a global inhibition of NFκB-mediated transcription of proangiogenic mediators.

4. TM was found to potentiate the effect of doxorubicin on inducing tumor cell apoptosis *in vitro* and *in vivo*.

Conclusions:

We have made significant progress in the past three years in understanding how TM acts as an anti-angiogenic compound. TM was found to be an indirect anti-angiogenic by inhibiting NFκB activity of tumor cells resulting in decreased secretion of NFκB-dependent pro-angiogenic factor. Moreover, TM was found to significantly enhance the effect of doxorubicin in inducing tumor cell apoptosis *in vitro* using annexin V and clonogenic cell survival assays and *in vivo* using an orthotopic model of breast cancer.

References:

1. Gilmore TD (1999) Oncogene, 18: 6842-6844.
2. Libermann TA and Baltimore D (1990) Mol. Cell Biol., 10: 2327-2334.
3. Kunsch C and Rosen CA (1993) Mol. Cell Biol., 13: 6137-6142.

4. van de Stolpe A, Caldenhoven E, Stade BG, Koenderman L, Raaijmakers JAM, Johnson JP, and van der Saag PT (1994) J. Biol. Chem., 269: 6185-6192.

5. Iademarco MF, McQuillan JJ, Rosen GD, and Dean DC (1992) J. Biol. Chem., 267: 16323-16329.

6. Novak U, Cocks BG, and Hamilton JA (1991) Nucleic Acids Res., 19: 3389-3393.

7. Huang S, Robinson JB, DeGuzman A, Bucana CD, and Fidler IJ (2000) Cancer Res., 60: 5334-5339.

Appendix:

Final Report Bibliography

1. **Pan Q**, Kleer CG, van Golen KL, Irani J, Bottema KM, Bias C, De Carvalho M, Mesri EA, Robins DM, Dick RD, Brewer GJ and Merajver SD (2002) Copper deficiency induced by tetrathiomolybdate suppresses tumor growth and angiogenesis. *Cancer Res.* 62:4854-4859.

2. **Pan Q**, Bao LW, Kleer CG, Brewer GJ, and Merajver SD (2003) Antiangiogenic tetrathiomolybdate enhances doxorubicin therapy against breast carcinoma. *Mol. Cancer Ther*. 2:617-622.

3. **Pan Q**, Bao LW, and Merajver SD (2003) Tetrathiomolybdate inhibits tumor angiogenesis and metastasis through suppression of the NFκB signaling cascade. *Mol. Cancer Res.* 1:701-706.

Personnel Paid From This Research Fellowship

1. Quintin Pan, Ph.D.

Advances in Brief

Copper Deficiency Induced by Tetrathiomolybdate Suppresses Tumor Growth and Angiogenesis[1]

Quintin Pan, Celina G. Kleer, Kenneth L. van Golen, Jennifer Irani, Kristen M. Bottema, Carlos Bias, Magda De Carvalho, Enrique A. Mesri, Diane M. Robins, Robert D. Dick, George J. Brewer,[2] and Sofia D. Merajver[2,3]

Department of Internal Medicine, Division of Hematology and Oncology [Q. P., K. L. v. G., J. I., K. M. B., G. J. B., S. D. M.], Departments of Pathology [C. G. K.] and Human Genetics [D. M. R., R. D. D., G. J. B.], and Comprehensive Cancer Center [Q. P., C. G. K., K. L. v. G., K. M. B., S. D. M.], University of Michigan Medical School, Ann Arbor, Michigan 48109, and Laboratory of Viral Oncogenesis, Division of Hematology and Oncology, Department of Medicine, Weill Medical College of Cornell University, New York, New York 10021 [C. B., M. D. C., E. A. M.]

Abstract

Copper plays an essential role in promoting angiogenesis. Tumors that become angiogenic acquire the ability to enter a phase of rapid growth and exhibit increased metastatic potential, the major cause of morbidity in cancer patients. We report that copper deficiency induced by tetrathiomolybdate (TM) significantly impairs tumor growth and angiogenesis in two animal models of breast cancer: an inflammatory breast cancer xenograft in nude mice and Her2/*neu* cancer-prone transgenic mice. *In vitro*, TM decreases the production of five proangiogenic mediators: (*a*) vascular endothelial growth factor; (*b*) fibroblast growth factor 2/basic fibroblast growth factor; (*c*) interleukin (IL)-1α; (*d*) IL-6; and (*e*) IL-8. In addition, TM inhibits vessel network formation and suppresses nuclear factor (NF)κB levels and transcriptional activity. Our study suggests that a major mechanism of the antiangiogenic effect of copper deficiency induced by TM is suppression of NFκB, contributing to a global inhibition of NFκB-mediated transcription of proangiogenic factors.

Introduction

Copper, an essential trace [3] element ubiquitous in the diets of humans, is an important cofactor for angiogenesis. Copper stimulates proliferation and migration of human endothelial cells (1, 2). Several reports showed a decrease in microvessel density and tumor size in penicillamine-treated, copper-deficient rabbits and rats xenografted with 9L gliosarcoma cells (3, 4). However, the molecular mechanism by which copper deficiency regulates angiogenesis remains unknown. To expedite and sustain the end point of clinical copper deficiency, we used a potent and novel copper chelator, TM,[4] developed for the treatment of Wilson's disease (5). Patients with Wilson's disease, a rare autosomal recessive disorder, have a metabolic defect of copper transport that results in life-threatening accumulation of copper in multiple organs, notably liver and the brain. TM forms a high-affinity tripartite complex with copper and albumin to chelate copper from the bloodstream. Copper status in mammals treated with TM cannot be reliably followed in the early stages of treatment by measuring total

serum copper levels because the complexed copper is still detected but is not bioavailable. Serum Cp, whose synthesis is directly regulated by the bio-availability of copper to the liver, is a more accurate indicator of copper status over a wide range and thus is used as a surrogate marker of total copper status. TM safely induced copper deficiency within 2–4 weeks in humans and mice. In a recent study, we showed that copper deficiency induced by TM significantly inhibited tumor growth of head and neck squamous cell carcinoma in severe combined immunodeficient mice (6). Evidence from Phase I and preliminary results from ongoing Phase II clinical trials demonstrate that humans can withstand significant copper deficiency induced by TM with Cp reduction to 20% of baseline (7).[5] Using three-dimensional ultrasound imaging, we demonstrated a reduction in blood flow to tumor masses in patients on TM therapy (7). This evidence supports the empiric link between copper deficiency induced by TM and inhibition of tumor angiogenesis in humans.

Materials and Methods

Cell Lines. HME cells were immortalized with human papilloma virus E6/E7 and grown in 5% fetal bovine serum (Sigma Chemical Co.) supplemented with Ham's F-12 medium (JRH Biosciences) containing insulin, hydrocortisone, epidermal growth factor, and cholera toxin (Sigma Chemical Co.). The SUM149 inflammatory breast cancer cell line was developed from a primary inflammatory breast cancer tumor and grown in 5% fetal bovine serum supplemented with Ham's F-12 medium containing insulin and hydrocortisone. The HME cells were characterized as being keratin-19 positive, ensuring that they are from the same differentiation lineage as the SUM149 inflammatory breast cancer cells.

Animal Models of Breast Cancer. SUM149 cells (1 × 10⁶ cells) were orthotopically injected into the upper left mammary fat pad of 10-week-old female athymic nude mice. Cells were trypsinized, washed, and resuspended in Hank's buffered saline solution (HBSS) at a density of 1 × 10⁶ cells/200 μl. Mice were anesthetized using 10 mg/ml ketamine, 1 mg/ml xylazine, and 0.01 mg/ml glycopyrrolate, and an incision below the thoracic left mammary fat pad was made. Using a 27-gauge needle, the cell suspension was injected into the exposed mammary fat pad, and the wound was closed with a single wound clip. After a brief recovery period, tumor-implanted mice were randomly assigned and gavaged with water (control; $n = 7$) or 0.7 mg/day TM ($n = 7$) daily for 7 weeks. Tumor volume was measured weekly and calculated as (length × width²)/2.

Mouse mammary tumor virus-Her2/*neu* transgenic mice were purchased from Jackson Laboratory. At ~100 days old, female mouse mammary tumor virus-Her2/*neu* mice were randomly assigned to two groups and gavaged with water (control; $n = 22$) or 0.75 mg/day TM ($n = 15$) for the entire experimental protocol. Mice were monitored weekly for overt palpable tumors, and disease-free survival curve was calculated using Log-rank analysis.

Quantification of Microvessel Density. Tumors from control or TM-treated mice were resected, immersion fixed in 10% buffered formalin, and

paraffin embedded. Intratumoral microvessel density was assessed with CD31 staining (DAKO) using the vascular hotspot technique. Sections were scanned at low power to determine areas of highest vascular density. Within this region, individual microvessels were counted in three separate random fields at high power ($\times$400 magnification). The mean vessel count from the three fields was used. A single countable microvessel was defined as any endothelial cell or group of cells that was clearly separate from other vessels, stroma, or tumor cells without the necessity of a vessel lumen.

Conditioned Media from SUM149 Cells. SUM149 cells were plated at a density of 2×10^5 cells in 100 mm^2 dishes. Cells were treated with vehicle or 0.1 nM TM for 72 h. Conditioned media was collected, centrifuged for 5 min at 2500 rpm, and divided into 1-ml aliquots. Quantikine human VEGF, basic FGF/FGF2, and IL-1α ELISAs (R&D Systems, Inc., Minneapolis, MN) were used to measure protein levels of the 165 amino acid species of VEGF, basic FGF/FGF2, and IL-1α. ELISAs for IL-6 and IL-8 were performed by the University of Maryland Cytokine Core Laboratory.[6]

Rat Aortic Ring Assay. Aorta was removed from a freshly sacrificed Sprague Dawley rat and rinsed in ice-cold HBSS containing penicillin and streptomycin. Segmental rings, $\sim$1 mm in width, were cut from the aorta and embedded in a 50-μl aliquot of 10 mg/ml Matrigel in six-well plates. Rings were incubated overnight at 37°C in serum-free media and then exchanged for conditioned media from control or TM-treated SUM149 cells. Subsequently, rings were incubated for 4 days at 37°C and analyzed by phase-contrast microscopy for microvessel outgrowth.

Transient Transfection and Reporter Gene Assay. SUM149 or HME cells (1×10^5) were transfected transiently with 1 μg of pNFκB (Clontech Laboratories, Inc.) and 0.05 μg pRL-TK (Clontech Laboratories, Inc.) with FuGene6 transfection reagent (Roche Biochemicals). pRL-TK, a *Renilla* luciferase vector, was cotransfected to normalize for transfection efficiency. After a 24-h recovery period, transfected cells were incubated in fresh medium with or without the addition of 2 nM CuSO$_4$. Cells were treated subsequently with vehicle, TM (1 nM), TNFα (2 pM), or TM and TNFα for 24, 48, or 72 h. Cells were harvested in passive lysis buffer, and the activities of the firefly luciferase and *Renilla* luciferase were quantified on a Monolight 2010 luminometer (Analytical Luminescence Laboratory) using the dual luciferase assay system (Promega Corp.).

Electrophoretic Mobility Shift Assay. Nuclear extracts from SUM149 cells were incubated with ^{32}P-labeled κB consensus sequence in a buffer containing 20 mM HEPES (pH 7.9), 20% glycerol, 100 mM KCl, 0.2 mM EDTA, 0.5 mM phenylmethylsulfonyl fluoride, and 0.5 mM DTT for 30 min at 25°C. Protein-DNA complexes were resolved on a high ionic strength 5% polyacrylamide gel containing 0.5 $\times$ Tris-borate EDTA buffer [380 mM glycine, 45 mM Tris base (pH 8.5), 45 nM boric acid, and 2 mM EDTA]. Supershift analysis was performed as described above except nuclear extracts were preincubated with p50, RelA, p52, c-Rel, or RelB antibody (Upstate Biotechnology) for 30 min on ice.

Western Blot Analysis. Proteins were harvested from SUM149 cells using radioimmunoprecipitation assay buffer (1 $\times$ PBS, 1% NP40, 0.5% sodium deoxycholate, 0.1% SDS, 0.1 mg/ml phenylmethylsulfonyl fluoride, 1 mM sodium orthovanadate, and 0.3 mg/ml aprotinin; Sigma Chemical Co.). Aliquots (20 μg) were mixed with Laemelli buffer, heat denatured for 3 min, separated by 10% SDS-PAGE, and transferred to polyvinylidene difluoride membrane. Nonspecific binding was blocked by overnight incubation with 2% BSA in Tris-buffered saline with 0.05% Tween 20 (Sigma Chemical Co.). Immobilized proteins were probed using antibodies specific for p50 or RelA (Upstate Biotechnology). Protein bands were visualized by enhanced chemiluminescence (Amersham-Pharmacia Biotech).

Results and Discussion

Systemic Treatment with TM Inhibits Tumor Growth and Angiogenesis in SUM149 Xenografts.

To assess the antiangiogenic action of TM *in vivo*, we used a xenograft model with a cell line derived from a patient with inflammatory breast cancer, chosen because of its highly aggressive and prominently angiogenic form of breast cancer (8). Inflammatory breast cancer is characterized by a

[6] Internet address: http://www.cytokinelab.com.

very rapid course, typically progressing within 6 months to cause the specific clinical manifestations of erythmea, skin modules, and nipple retraction caused by tumor infiltration of lympathic and connective tissue (9, 10). Even with multimodality treatment, the 5-year disease-free survival is <45%, making inflammatory breast cancer the most aggressive and deadly form of locally advanced breast cancer (10). SUM149 inflammatory breast cancer cells (1×10^6) were orthotopically transplanted into the mammary fat pads of 10-week-old female athymic nude mice. Mice were gavaged with water (control) or 0.7 mg/day TM starting on the day of xenograft transplantation. Cp was followed weekly and used as a surrogate marker for serum copper status. After 1 week of treatment, Cp levels of TM-treated mice were maintained at 19 $\pm$ 4% of baseline for the remainder of the experiment. The size of primary breast tumors was potently suppressed by 69 $\pm$ 3% ($P < 0.001$, $n = 7$) as a result of systemic TM therapy (Fig. 1A). Tumors in the control group were highly vascularized as shown by immunohistochemical staining with a CD31 antibody (Fig. 1B). In contrast, the smaller tumors resected from TM-treated mice were only sparsely vascularized (mean vessel count; 16 $\pm$ 2 *versus* 26 $\pm$ 3,

Control   TM

Fig. 1. Systemic treatment with TM inhibits tumor growth and angiogenesis in SUM149 xenografts. *A*, tumor growth of SUM149 xenografts. SUM149 inflammatory breast cancer cells (1×10^6) were orthotopically injected into the upper left mammary fat pad of 10-week-old athymic female mice. Mice were gavaged with water (*Control*) or 0.7 mg/day TM starting on the day of xenograft injection. Tumor volume was measured weekly and calculated as (length $\times$ width^2)/2. $*P < 0.01$, $**P < 0.001$; $n = 7$. *B*, microvessel density of SUM149 xenografts. Breast tumors from control or TM-treated mice were resected and stained with anti-CD31 antibodies. Mean vessel count was 26 $\pm$ 3 in tumors from control mice and 16 $\pm$ 2 in tumors from TM-treated mice. $P < 0.04$; $n = 3$.

A

B

Conditioned-Media From
Control Cells

Conditioned-Media From
TM-treated Cells

TM added to Conditioned-
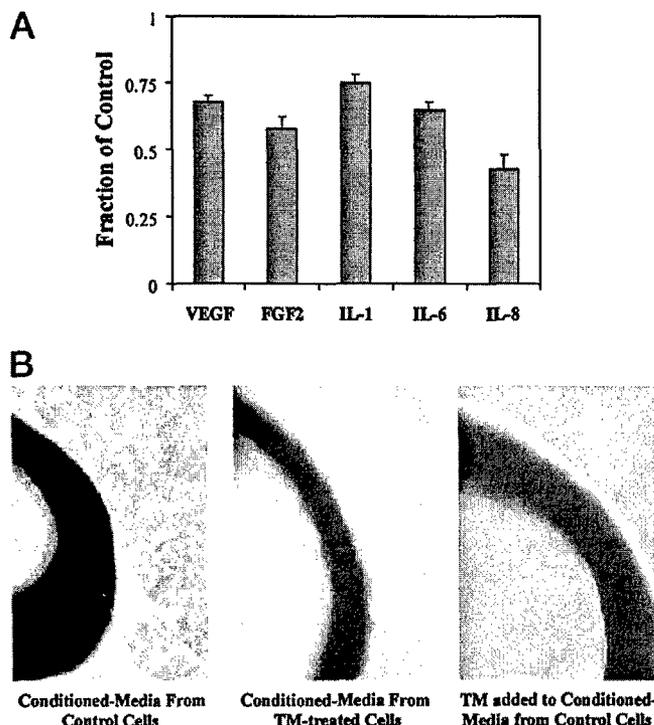Media from Control Cells

Fig. 2. TM decreases proangiogenic mediators and inhibits *in vitro* angiogenesis. *A*, levels of proangiogenic mediators in conditioned medium from SUM149 cells. Conditioned media from control and TM-treated (0.1 nM) SUM149 cells were analyzed for VEGF, FGF2, IL-1α, IL-6, and IL-8 by ELISA. Data are presented as a fraction of control SUM149 cells. *B*, rat aortic ring assay. Segments of rat aorta were embedded in Matrigel and incubated in the corresponding conditioned media for 4 days at 37°C. Microvessel outgrowth was analyzed by phase-contrast microscopy. Data are representative of three independent experiments.

$P < 0.04$, $n = 3$), providing further evidence that copper deficiency induced by TM is antiangiogenic.

TM Decreases Proangiogenic Mediators and Inhibits *in Vitro* Angiogenesis. A possible explanation for the antiangiogenic action of TM is that copper deficiency induced by TM may result in a shift of overall balance toward inhibition of angiogenesis as a consequence of a decrease in proangiogenic factors, increase in antiangiogenic factors, or a combination of both. Consistent with this hypothesis, TM-treated SUM149 cells released significantly lower amounts of five potent proangiogenic mediators: (*a*) VEGF; (*b*) FGF2; (*c*) IL-1α; (*d*) IL-6; and (*e*) IL-8 ($P < 0.05$; Fig. 2*A*). Moreover, IL-6 and IL-8 mRNA expression was decreased by TM (data not shown). To test whether the decrease in proangiogenic mediators was sufficient to impair the angiogenic potential of the conditioned media, we used the rat aortic ring assay, an *in vitro* model of angiogenesis that resembles the outgrowth of primordial vessels from a host vessel under an

appropriate stimulus (Fig. 2*B*). Rat aortic rings incubated with conditioned media from TM-treated SUM149 cells showed a marked reduction in vessel outgrowth when compared with rings incubated with conditioned medium from untreated SUM149 cells. In addition, primordial blood vessels failed to grow when conditioned media from untreated SUM149 cells were supplemented with TM before incubation with aortic rings. Because copper may be involved in the regulation of the biological activity of the prototype members of the FGF gene family (11), we tested if copper deficiency could suppress the stimulatory effect of exogenous FGF2 on HUVECs. TM blocked FGF2-stimulated HUVEC tubule formation in a dose-dependent manner, without affecting HUVEC proliferation (data not shown). Although previous studies have suggested that copper may be required for endothelial cell proliferation and migration (1, 2), our study indicates, for the first time, that absence of copper is able to block exogenous FGF2-mediated organization of endothelial cells into a primordial vessel network. Our data demonstrate that copper deficiency inhibits tumor angiogenesis by two different mechanisms: (*a*) reduction in the level of extracellular proangiogenic mediators released by cancer cells; and (*b*) inhibition of endothelial cell differentiation.

TM Suppresses NFκB Protein Levels and Transcription. Evidence linking uncontrolled NFκB activity to oncogenesis has emerged in recent years. The NFκB transcription factor is known to regulate genes important for invasion, angiogenesis, and metastasis. These include proangiogenic factors, such as VEGF, IL-6, and IL-8, matrix metalloproteinases, urokinase plasminogen activator, and cell adhesion molecules, such as intercellular adhesion molecule-1 and vascular cell adhesion molecule-1 (12–16). Recently, blocking NFκB activity in human ovarian cancer cells was reported to inhibit VEGF and IL-8 expression, resulting in a decrease in tumor angiogenesis (17). To investigate the NFκB dependence of proangiogenic factors in SUM149 cells, we transfected these cells with the super-repressor IκBα (S32AS36A). Conditioned media from SUM149 super-repressor IκBα clones had significantly lower amounts of VEGF, IL-6, and IL-8 in comparison with the empty vector-transfected SUM149 cells; 45 ± 5% inhibition for VEGF, 37 ± 4% inhibition for IL-6, and 58 ± 5% inhibition for IL-8 ($P < 0.05$, $n = 3$). Because TM was able to decrease these proangiogenic factors to a similar extent, we sought to determine whether copper deficiency induced by TM is modulating NFκB-mediated signaling. SUM149 and nontumorigenic-immortalized HME cells were transiently transfected with pNFκB, a vector that contains four tandem copies of the κB consensus sequence upstream of the luciferase reporter gene (Fig. 3). Endogenous NFκB activity was shown to be 2.5-fold higher in SUM149 cells in comparison with HME cells. This is consistent with our observation that p50 protein levels were significantly higher in SUM149 cells (data not shown). Several studies using human breast cancer cells also reported that overexpression of p50 results in constitutive NFκB activity (18, 19).

Fig. 3. TM suppresses NFκB-dependent transcription. SUM149 or HME cells were transfected with pNFκB (Clontech Laboratories, Inc.), a vector that contains four tandem copies of the κB consensus sequence fused to a TATA-like promoter region from the herpes simplex virus thymidine kinase promoter. pRL-TK (Promega Corp.), a *Renilla* luciferase vector, was cotransfected into the cells to normalize for transfection efficiency. After a 24-h recovery period, transfected cells were incubated in fresh medium with or without the addition of 2 nM CuSO₄. Cells were treated subsequently with vehicle, TM (1 nM), TNFα (2 pM), or TM and TNFα for 24 h. *P < 0.001; $n = 6$, vehicle *versus* TM. **P < 0.001; $n = 6$, vehicle or TNFα *versus* TM + TNFα.

A   **B**

TM: - + +   Antibody: p50 RelA p52 c-Rel RelB

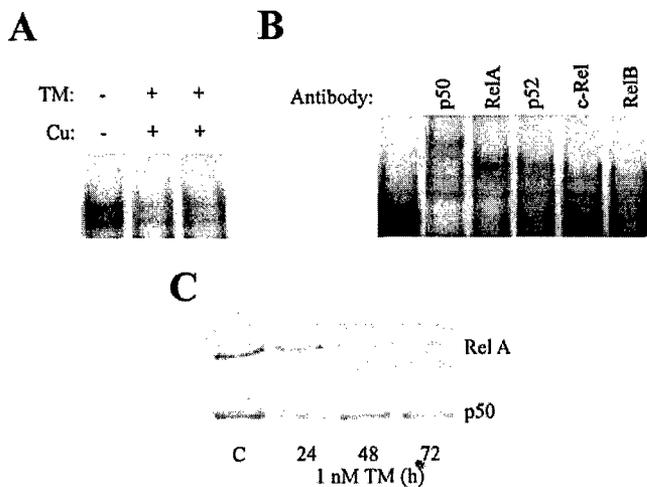Cu: - + +

C

Rel A

p50

C   24   48   72

1 nM TM (h)
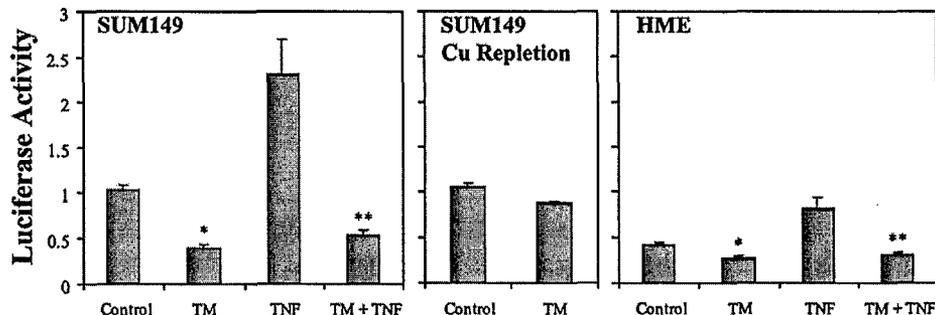
Fig. 4. TM decreases NFκB binding and protein levels. *A*, gel shift analysis. SUM149 cells were treated with vehicle or TM (1 nM) with or without the addition of 2 nM CuSO₄ for 72 h. Nuclear proteins were extracted, incubated with ³²P-labeled κB consensus sequence, and resolved by EMSA. *B*, identification of NFκB binding complex. Supershift analysis was performed by preincubating nuclear extracts with p50, RelA, p52, c-Rel, or RelB antibody (Upstate Biotechnology) for 20 min on ice. *C*, p50 and RelA protein levels. SUM149 cells were treated with vehicle or TM (1 nM) for 72 h. p50 and RelA levels were determined by Western blot analysis. Data are representative of three independent experiments.

After treatment for 24 h, TM inhibited luciferase activity by 62 ± 2% (P < 0.001, n = 6) in SUM149 cells and 34 ± 2% (P < 0.001, n = 3) in HME cells. Moreover, TM completely blocked TNFα-stimulated NFκB activity in both cell lines. Similar results were observed at 48 and 72 h demonstrating that TM is also able to inhibit NFκB activity on a sustained basis without affecting cell survival under these conditions. In Fig. 4A, we analyzed the binding of nuclear proteins from SUM149 cells to a labeled oligonucleotide spanning the κB consensus sequence. Extracts from TM-treated cells showed a decrease in nuclear protein binding to the κB consensus sequence. In addition, supershift analysis revealed that the predominant NFκB components in SUM149 cells are p50, p52, and RelA. When cells were cultured with added copper (2 nM CuSO₄ addition), TM partially lost its ability to regulate κB binding and NFκB transcriptional activity. In addition, copper repletion partially reversed TM inhibition of IL-6 and IL-8 mRNA expression (data not shown), consistent with restoring NFκB's ability to enhance transcription of these genes. Interestingly, p50 and RelA protein levels were reduced after treatment with TM in SUM149 cells, suggesting that TM may be suppressing NFκB activity by decreasing levels of NFκB component proteins.

Our data clearly demonstrate that NFκB signaling is suppressed after TM treatment *in vitro*. Because VEGF, IL-6, and IL-8 are NFκB-regulated genes, we anticipate that the decreased secretion of these proteins may be a direct consequence of TM's ability to inhibit NFκB activity. This leads to the suggestion that TM is limiting tumor neovascularization by repressing the ability of cancer cells to release NFκB-dependent inflammatory cytokines and proangiogenic mediators into the extracellular compartment and thus limiting the autocrine and/or paracrine effects of these proteins to stimulate angiogenesis in the tumor microenvironment. TM also retards the release of IL-1α in SUM149 cells. Consistent with our observation, the release of IL-1α is dependent on the oxidative function of intracellular copper and blocked with TM treatment.[7] Interestingly, IL-1α was reported to

---

[7] A. Mandinova, S. Bellum, C. Bagala, R. Soldi, I. Micucci, M. Landriscina, F. Tarantini, I. Prudovsky, and T. Maciag. The stress-induced release of the pro-inflammatory cytokine IL1α is Cu²⁺-dependent. Proc. Natl. Acad. Sci. USA, submitted for publication, 2002.

enhance NFκB activity resulting in an increase in IL-6 (20). IL-1 is able to induce the expression of VEGF and FGF2 in human endothelial and melanoma cells (21, 22). From these observations, we further hypothesize that TM may be limiting tumor angiogenesis by directly blocking the release of IL-1α from tumor cells to prevent additional NFκB stimulation in tumor and endothelial cells in close proximity.

TM Prevents the Development of *de Novo* Clinically Overt Tumors in Her2/*neu* Transgenic Mice. Our results suggest that the inhibition of proangiogenic factors within the tumor microenvironment accompanies copper deficiency. This leads to the corollary that malignant clones that arise in a copper-deficient milieu may not be able to stimulate sufficient neovascularization for growth beyond a few millimeters. We designed an experimental protocol to determine the effectiveness of TM in retarding or preventing the growth of mammary tumors in female Her2/*neu* transgenic mice. Extensive clinical studies have shown that overexpression of Her2/*neu* in patients with breast cancer correlates overall with poorer prognoses (23, 24). Female Her/*neu* mice develop focal mammary adenocarcinomas, which eventually metastasize to the lungs (25). These mice develop single or multifocal mammary tumors approximately at 205 days of age (25). By initiating TM treatment 90–120 days before tumors became clinically evident, we surmised that the TM-treated mice would be copper deficient throughout the key period of tumor development when angiogenesis is required for continued tumor growth. Female Her2/*neu* transgenic mice (~100 days old) were gavaged with water (control) or 0.75 mg/day TM (n = 22 for control group and n = 15 for TM group). Cp levels were maintained at 10–30% of baseline for the entire protocol. Depending on the individual mouse, 2–4 weeks were required to achieve the anticipated end point of copper depletion. We chose this end point to investigate whether the level of copper deficiency that would be tolerable in humans could inhibit the angiogenic switch in Her2/*neu* mice. TM-treated and control mice did not differ in weight or general health as evidenced by social behavior and level of activity. Fig. 5A depicts the Kaplan-Meier plot for disease-free survival of TM-treated and control mice. By 218 days, 50% of the control mice and none of the TM-treated mice had overt tumors. Log-rank analysis demonstrated that the TM-treated mice had a statistically significant prolongation of disease-free survival compared with the control group (P < 0.0147). At the conclusion of the experiment, with a median follow-up time of 221 days, palpable tumors were not observed in the TM-treated mice that remained copper deficient with Cp levels ≤30% of baseline. However, when TM-treated mice were released from therapy, measurable tumors were observed by 13 ± 5 (n = 5) days postrelease. The restoration of copper in these mice, previously copper deficient for >7 months, appears to be sufficient to enable tumor growth to proceed at the normal rate within 2 weeks. Therefore, it is clear that these TM-treated Her2/*neu* mice retained the capacity to develop macroscopic mammary tumors, and copper deficiency appears to act as a barrier for their appearance. It is important to note that Her2/*neu*-positive breast cancer cells have enhanced NFκB activity (26, 27). In light of our observations, this implies that in a copper-deficient environment, nascent breast cancer tumors with Her2/*neu* overexpression have impaired ability to activate the angiogenic switch attributable, in part, to decreased production of proangiogenic factors, perhaps as a consequence of NFκB inhibition by TM.

To investigate the effects of chronic TM administration on the mammary gland, we analyzed mammary gland whole mounts and the microscopic characteristics of tumors resected from the Her2/*neu* mice. Mammary glands of TM-treated Her2/*neu* mice showed regions containing multiple thickened end buds (Fig. 5B2). These large buds were widespread throughout the mammary glands of TM-treated Her2/*neu* mice. Histological analyses of these structures clearly
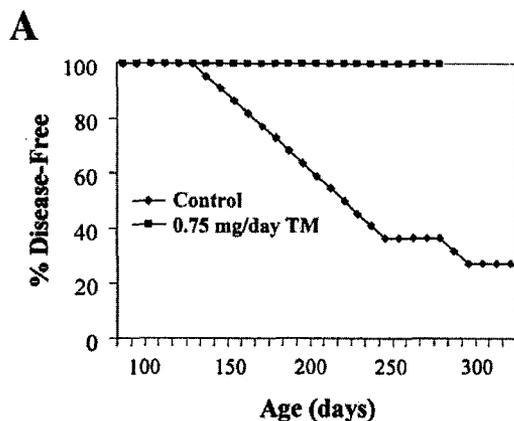
Fig. 5. TM prevents the development of *de novo* clinically overt tumors in Her2/*neu* transgenic mice. *A*, time to first tumor in Her2/*neu* transgenic mice. Female Her2/*neu* transgenic mice (~100 days old) were gavaged with water (*Control*) or 0.75 mg/day TM (*n* = 22 for vehicle group and *n* = 15 for TM treatment group). Cp levels were maintained at 10–30% of baseline for the entire experiment. Mice were monitored for the appearance of overt tumors, and disease-free survival was analyzed using Kaplan-Meier plot. *B*, whole mammary gland mounts. Mammary glands from control (*B1*) or TM-treated (*B2*) mice were fixed in a mixture of one part glacial acetic acid and three parts 100% ethanol for 60 min. The glands were washed for 15 min in 70% ethanol and rinsed with distilled water for 5 min. Whole mammary gland mounts were stained with alum carmine overnight and washed with 70, 90, and 100% ethanol for 15 min each. Subsequently, the mounts were washed with toluene for 15 min and stored in methyl salicylate. *C*, microscopic analysis of H&E-stained whole mammary gland mount. *C1*, control Her2/*neu* mouse (×100 magnification). *C2*, TM-treated Her2/*neu* mouse (×100 magnification). *C3*, TM-treated/release Her2/*neu* mouse (×100 magnification).
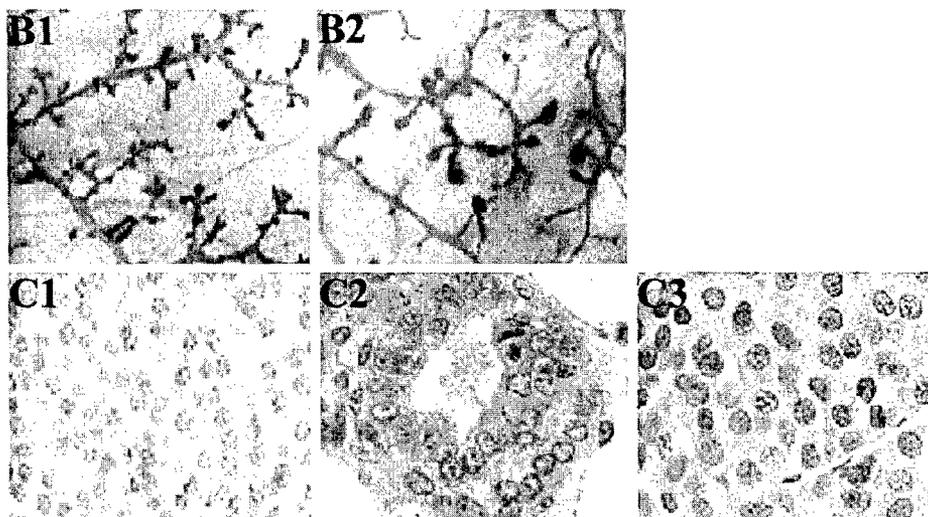
showed several discrete microscopic foci of hyperplastic or neoplastic epithelium interspersed among scant normal ducts lined by a single layer of normal cells. These foci contained pleomorphic cells, with increased cytoplasmic clearing and some prominent reddish nucleoli, often filling the duct entirely. These neoplastic foci also were observed in the mammary glands of vehicle-treated and TM-treated/ release Her2/*neu* mice. The rapid development of overt tumors in mice released from TM treatment strongly suggests that the cells of the microtumors in TM-treated mice are neoplastic. Interestingly, the morphology of the cells from the microtumors of TM-treated mice is strikingly similar to the cells from the bulky tumors that developed in vehicle- or TM-treated mice that were released from therapy (Fig. 5*C1-3*). This observation further supports our supposition that these microtumors are comprised of completely transformed cells, but failed to acquire neovascularization, and thus have remained noninvasive and relatively contained in a dormant state with minimal or no angiogenesis.

Taken together, these results support our initial clinical observations indicating that copper deficiency induced by TM is a potent approach to inhibit tumor angiogenesis with minimal adverse effects. TM exerts its antiangiogenic action at least in part through restriction of the extracellular appearance of proangiogenic factors and suppression of NFκB activity. The observation that TM suppresses NFκB activity is potentially exciting from a clinical perspective because constitutive NFκB activity is linked to the development of resistance to chemotherapy or radiotherapy (28, 29). Inhibition of NFκB by TM, in turn, may restore the sensitivity of resistant cancer cells and

recapitulate the efficacy of chemotherapy or radiotherapy-induced apoptosis. Moreover, the strong suppressive effect on tumor growth when the angiogenic switch is inhibited before or at the time of neoplastic transformation in mammary epithelium suggests a promising role for TM as a chemopreventative agent for use in carriers of cancer susceptibility genes.

References

1. Hu, G. F. Copper stimulates proliferation of human endothelial cells under culture. J. Cell. Biochem., *69:* 326–335, 1998.
2. McAuslan, B. R., and Reilly, W. Endothelial cell phagokinesis in response to specific metal ions. Exp. Cell Res., *130:* 147–157, 1980.
3. Brem, S. S., Zagzag, D., Tsanaclis, A. M., Gately, S., Elkouby, M. P., and Brien, S. E. Inhibition of angiogenesis and tumor growth in the brain. Suppression of endothelial cell turnover by penicillamine and the depletion of copper, an angiogenic cofactor. Am. J. Pathol., *137:* 1121–1142, 1990.
4. Yoshida, D., Ikeda, Y., and Nakazawa, S. Quantitative analysis of copper, zinc and copper/zinc ration in selected human brain tumors. J. Neuro-Oncol., *16:* 109–115, 1993.
5. Brewer, G. J., Dick, R. D., Yuzbasiyan-Gurkin, V., Tankanow, R., Young, A. B., and Kluin, K. J. Initial therapy of patients with Wilson's disease with tetrathiomolybdate. Arch. Neurol., *48:* 42–47, 1991.
6. Cox, C., Teknos, T. N., Barrios, M., Brewer, G. J., Dick, R. D., and Merajver, S. D. The role of copper suppression as an antiangiogenic strategy in head and neck squamous cell carcinoma. Laryngoscope, *111:* 696–701, 2001.
7. Brewer, G. J., Dick, R. D., Grover, D. K., LeClaire, V., Tseng, M., Wicha, M., Pienta, K., Redman, B. G., Jahan, T., Sondak, V. K., Strawderman, M., LeCarpentier, G., and Merajver, S. D. Treatment of metastatic cancer with tetrathiomolybdate, an anticopper, antiangiogenic agent: phase I study. Clin. Cancer Res., *6:* 1–10, 2000.
8. van Golen, K. L., Wu, Z. F., Qiao, X. T., Bao, L. W., and Merajver, S. D. RhoC GTPase overexpression modulates induction of angiogenic factors in breast cells. Neoplasia, *2:* 418–425, 2000.
9. Jaiyesimi, I., Buzdar, A., and Hortobagyi, G. Inflammatory breast cancer: a review. J. Clin. Oncol., *10:* 1014–1024, 1992.

10. Beahrs, O., Henson, D., and Hutter, R. (eds.). Manual for Staging Cancer, Ed. 3, pp. 145–150. Philadelphia, PA: Lippincott Williams and Wilkins, 1988.
11. Engleka, K. A., and Maciag, T. Inactivation of human fibroblast growth factor-1 (FGF-1) activity by interaction with copper ions involves FGF-1 dimer formation induced by copper-catalyzed oxidation. J. Biol. Chem., 267: 11307–11315, 1994.
12. Libermann, T. A., and Baltimore, D. Activation of interleukin-6 gene expression through the NF-κ B transcription factor. Mol. Cell. Biol., 10: 2327–2334, 1990.
13. Kunsch, C., and Rosen, C. A. NF-κ B subunit-specific regulation of the interleukin-8 promoter. Mol. Cell. Biol., 13: 6137–6146, 1993.
14. van de Stolpe, A., Caldenhoven, E., Stade, B. G., Koenderman, L., Raaijmakers, J. A., Johnson, J. P., and van der Saag, P. T. 12-O-tetradecanoylphorbol-13-ace. J. Biol. Chem., 269: 6185–6192, 1994.
15. Iademarco, M. F., McQuillan, J. J., Rosen, G. D., and Dean, D. C. Characterization of the promoter for vascular cell adhesion molecule-1 (VCAM-1). J. Biol. Chem., 267: 16323–16329, 1992.
16. Novak, U., Cocks, B. G., and Hamilton, J. A. A labile repressor acts through the NFkB-like binding sites of the human urokinase gene. Nucleic Acids Res., 19: 3389–3393, 1991.
17. Huang, S., Robinson, J. B., DeGuzman, A., Bucana, C. D., and Fidler, I. J. Blockade of nuclear factor-κB signaling inhibits angiogenesis and tumorigenicity of human ovarian cancer cells by suppressing expression of vascular endothelial growth factor and interleukin 8. Cancer Res., 60: 5334–5339, 2000.
18. Sovak, M. A., Bellas, R. E., Kim, D. W., Zanieski, G. J., Rogers, A. E., Traish, A. M., and Sonenshein, G. E. Aberrant nuclear factor-κB/Rel expression and the pathogenesis of breast cancer. J. Clin. Investig., 100: 2952–2960, 1997.
19. Nakshatri, H., Bhat-Nakshatri, P., Martin, D. A., Goulet, R. J., Jr., and Sledge, G. W., Jr. Constitutive activation of NF-κB during progression of breast cancer to hormone-independent growth. Mol. Cell. Biol., 17: 3629–3639, 1997.
20. Bhat-Nakshatri, P., Newton, T. R., Goulet, R., Jr., and Nakshatri, H. NF-κB activation and interleukin 6 production in fibroblasts by estrogen receptor-negative breast cancer cell-derived interleukin 1α. Proc. Natl. Acad. Sci. USA, 95: 6971–6976, 1998.
21. Torisu, H., Ono, M., Kiryu, H., Furue, M., Ohmoto, Y., Nakayama, J., Nishioka, Y., Sone, S., and Kuwano, M. Macrophage infiltration correlates with tumor stage and angiogenesis in human malignant melanoma: possible involvement of TNFα and IL-1α. Int. J. Cancer, 85: 182–188, 2000.
22. Ko, Y., Totzke, G., Gouni-Berthold, I., Sachinidis, A., and Vetter, H. Cytokine-inducible growth factor gene expression in human umbilical endothelial cells. Molecular and Cellular Probes, 13: 203–211, 1999.
23. Slamon, D. J., Clark, G. M., Wong, S. G., Levin, W. J., Ullrich, A., and McGuire, W. L. Human breast cancer: correlation of relapse and survival with amplification of the HER-2/neu oncogene. Science (Wash. DC), 235: 177–182, 1987.
24. Paterson, M. C., Dietrich, K. D., Danyluk, J., Paterson, A. H. G., Lees, A. W., Jamil, N., Hanson, J., Jenkins, H., Krause, B. E., and McBlain, W. A. Correlation between c-rebB-2 amplification and risk of recurrent disease in node-negative breast cancer. Cancer Res., 51: 556–567, 1991.
25. Guy, C. T., Webster, M. A., Schaller, M., Parsons, T. J., Cardiff, R. D., and Muller, W. J. Expression of the neu protooncogene in the mammary epithelium of transgenic mice induces metastatic disease. Proc. Natl. Acad. Sci. USA, 89: 10578–10582, 1992.
26. Galang, C. K., Garcia-Ramirez, J., Solski, P. A., Westwick, J. K., Der, C. J., Neznanov, N. N., Oshima, R. G., and Hauser, C. A. Oncogenic Neu/ErbB-2 increases ets. AP-1, and NF-κB-dependent gene expression, and inhibiting ets activation blocks Neu-mediated cellular transformation. J. Biol. Chem., 271: 7992–7998, 1996.
27. Zhou, B. P., Hu, M. C., Miller, S. A., Yu, Z., Xia, W., Lin, S. Y., and Hung, M. C. HER-2/neu blocks tumor necrosis factor-induced apoptosis via the Akt/NF- kappaB pathway. J Biol Chem, 275: 8027–8031, 2000.
28. Wang, C. Y., Cusack, J. C., Jr., Liu, R., and Baldwin, A. S., Jr. Control of inducible chemoresistance: enhanced anti-tumor therapy through increased apoptosis by inhibition of NF-κB. Nat. Med., 5: 412–417, 1999.
29. Wang, C. Y., Mayo, M. W., and Baldwin, A. S., Jr. TNF- and cancer therapy-induced apoptosis: potentiation by inhibition of NF-κB. Science (Wash. DC), 274: 784–787, 1996.

Antiangiogenic Tetrathiomolybdate Enhances the Efficacy of Doxorubicin against Breast Carcinoma[1]

Quintin Pan, Li Wei Bao, Celina G. Kleer, George J. Brewer, and Sofia D. Merajver[2]

Department of Internal Medicine, Division of Hematology and Oncology [Q. P., L. W. B., G. J. B., S. D. M.], Departments of Pathology [C. G. K.] and Human Genetics [G. J. B.], and Comprehensive Cancer Center [Q. P., L. W. B., C. G. K., S. D. M.], University of Michigan Medical School, Ann Arbor, Michigan 48109

Abstract

Constitutive activation of nuclear factor κB is implicated to be a critical survival mechanism used by carcinoma cells to escape apoptosis. Tetrathiomolybdate (TM), a novel copper chelator, exhibits potent antiangiogenic properties, in part, through suppression of the nuclear factor κB signaling cascade. In this study, we determined whether TM enhances doxorubicin-induced apoptosis in SUM149 inflammatory breast carcinoma cells. Apoptosis was not observed in these cells after TM treatment. Moreover, SUM149 cells were relatively resistant to doxorubicin-induced apoptosis ranging from 9.9 $\pm$ 2.9% to 21.5 $\pm$ 2.0% apoptotic cells for 0.1 to 2.5 μM doxorubicin treatment. A greater-than-additive increase (33.8 $\pm$ 4.6%, 57.5 $\pm$ 5.2%, or 83.7 $\pm$ 1.0% apoptosis with TM and 0.1, 0.5, or 2.5 μM doxorubicin, respectively) in apoptosis was observed in cells treated with the combination therapy of TM and doxorubicin. In SUM149 xenografts, TM and doxorubicin significantly retarded tumor growth in comparison with either agent administered alone ($P < 0.03$). Tumor cell apoptosis in the combination therapy-treated mice was 113.3 $\pm$ 20% greater than that in TM-treated mice and 52.4 $\pm$ 14.3% greater than that in doxorubicin-treated mice. These results suggest that TM may enhance the rate of pathological complete response when used in combination with an anthracycline in neoadjuvant therapy of breast carcinoma.

Introduction

The NF-κB[3]/Rel family of transcription factors is comprised of RelA, RelB, c-Rel, p50 (nfκb1), and p52 (nfκb2; Ref. 1). Numerous reports have characterized various types of solid tumors, including breast, ovarian, colon, pancreatic, thyroid, bladder, and prostate tumors, with deregulated NF-κB activity as a result of constitutive activation of the NF-κB signaling pathway or inactivating mutations of IκB protein members (2–6). Overexpression of p50 and p52 has been observed in colon, prostate, and breast carcinomas (5, 6). Several studies using human breast carcinoma cells have shown that overexpression of p50 results in constitutive NF-κB activity (5, 6). Subsequently, constitutive NF-κB activation was shown to correlate with the conversion of breast carcinoma cells to hormone-independent growth, a hallmark of a more aggressive and metastatic phenotype (5). Taken together, these reports indicate that activation of NF-κB appears to be an event that frequently occurs during malignant transformation and progression of HME cells and other cell types.

There is increasing evidence that deregulated NF-κB activation is linked to the development of resistance to cytotoxic therapy. Tumors with elevated levels of NF-κB are resistant to apoptosis induced by chemotherapy and radiotherapy (7). Several groups reported that inhibition of NF-κB activation increased the sensitivity of resistant carcinoma cells to apoptosis-inducing stimuli (6, 8, 9). TM, a copper chelator, has proven to be a potent antiangiogenic compound in animals and humans (10–13). Recently, TM was found to be an inhibitor of NF-κB activity in SUM149 inflammatory breast carcinoma cells (11). This observation is exciting from a clinical perspective because it suggests that TM may be able to enhance the efficacy of chemotherapeutics against cancers with NF-κB overexpression. In this study, the combination therapy of TM and doxorubicin was more effective at inducing apoptosis and suppressing tumor growth in NF-κB-overexpressing SUM149 cells than either agent administered alone. Our data indicate that TM can enhance the efficacy of doxorubicin and thus suggest a testable clinical hypothesis of using TM in combination with an anthracycline in neoadjuvant therapy of primary or refractory tumors.

Materials and Methods

Cell Line. The SUM149 inflammatory breast carcinoma cell line was developed from a primary inflammatory breast carcinoma nodule and was grown in Ham's F-12 medium sup-

---

[3] The abbreviations used are: NF-κB, nuclear factor κB; TM, tetrathiomolybdate; HME, human mammary epithelial.
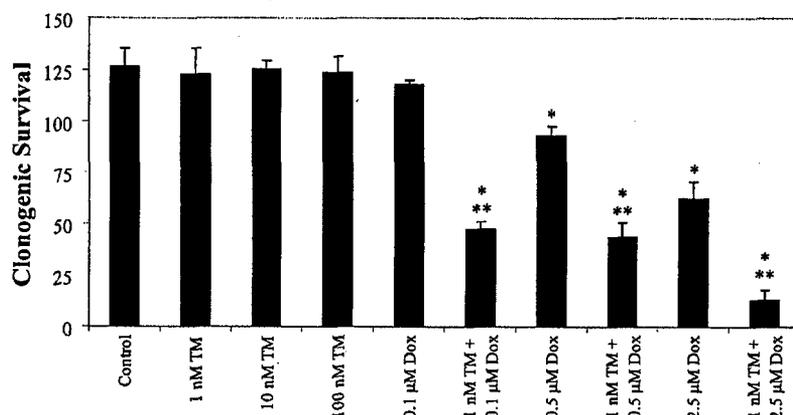
A
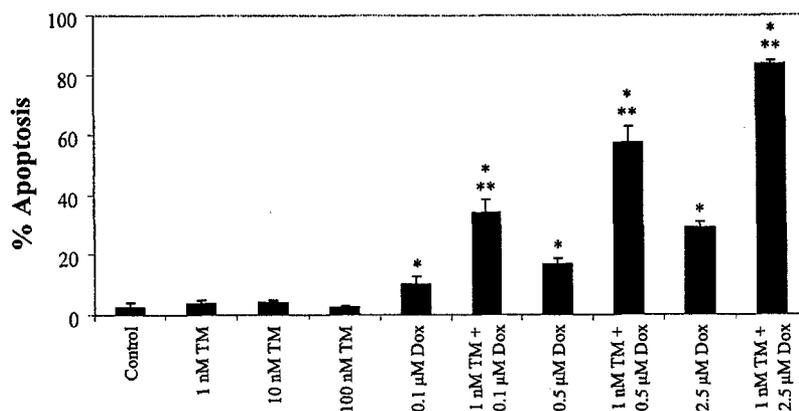
B

Fig. 1. Combination therapy of TM and doxorubicin enhances apoptosis and decreases clonogenic survival. *A,* flow cyotometric analysis of apoptosis. SUM149 cells were treated with control, TM (1, 10, or 100 nM), doxorubicin (0.1, 0.5, or 2.5 μM), or TM (1 nM) and doxorubicin (0.1, 0.5, or 2.5 μM) for 72 h. Apoptosis was determined by the FITC-Annexin V/propidium iodide assay. Data are presented as mean ± SE. *, $P < 0.01$ *versus* control; **, $P < 0.005$ *versus* appropriate single-agent doxorubicin treatment. *B,* clonogenic survival. SUM149 cells were treated with control, TM (1, 10, or 100 nM), doxorubicin (0.1, 0.5, or 2.5 μM), or TM (1 nM) and doxorubicin (0.1, 0.5, or 2.5 μM) for 72 h. After 14 days, cells were stained with trypan blue and counted. Data are presented as mean number of clones ± SE. *, $P < 0.02$ *versus* control; **, $P < 0.003$ *versus* appropriate single-agent doxorubicin treatment.

plemented with 5% fetal bovine serum, insulin, and hydrocortisone (14).

Detection of Apoptotic Cells. SUM149 cells (2.5 × 10⁵) were plated on 100-mm dishes and allowed to grow for 24 h. Subsequently, cells were treated with vehicle (control), TM, doxorubicin, or TM and doxorubicin for 72 h. Cells were harvested, washed with cold PBS, and costained with Annexin V and propidium iodide according to the manufacturer's protocol (ApoAlert Annexin V-FITC Apoptosis Kit; Clontech). Apoptotic cells were analyzed on a FACScan flow cytometer.

Clonogenic Survival Assay. SUM149 cells (250 cells) were plated on 6-well plates and allowed to grow for 24 h. Subsequently, cells were treated with vehicle (control), TM, doxorubicin, or TM and doxorubicin for 72 h. Cells were washed with PBS, and fresh medium was replaced as needed for 14 days. Clones were fixed with methanol and acetic acid, stained with trypan blue dye, and counted.

Orthotopic Xenograft Model of Breast Cancer. SUM149 (1 × 10⁶) cells were orthotopically injected in the upper left mammary pad of 10-week-old female athymic nude mice (Harlan). Cells were trypsinized, washed, and resuspended in HBSS at a density of 1 × 10⁶ cells/100 μl.

Mice were anesthetized using 10 mg/ml ketamine, 1 mg/ml xylazine, and 0.01 mg/ml glycopyrrolate, and an incision below the thoracic left mammary fat pad was made. Using a 27-gauge needle, the cell suspension was injected into the exposed mammary fat pad, and the wound was closed with a single wound clip. Mice were monitored daily, and tumor size was measured using a microcaliper. Tumor volume was calculated using the following formula: (length × width²)/2.

Immunohistochemistry and Quantitation of Microvessel Density and Apoptosis. Mammary gland tumors harvested at autopsy were fixed in formalin and processed for immunostaining. Intratumoral microvessel density was assessed with CD31 staining (PharMingen) using the vascular hot spot technique (15). Sections were scanned at low power to determine areas of highest vascular density for quantitative assessment. Within this region, individual microvessels were counted in 10 separate random fields at high power (×400 magnification), and the mean vessel count from the 10 fields was calculated. A single countable microvessel was defined as any endothelial cell or group of cells that was clearly separate from other vessels, stroma, or tumor cells without the necessity of a vessel lumen. Intratumoral apoptosis was assessed using the ApopTag kit (Intergen). Sec-

tions were scanned at low power to determine areas of highest apoptotic cell density for quantitative assessment. Within this region, the number of apoptotic cells per 500 total cells was counted in 5 separate random fields at high power (×400), and the total percentage of apoptotic cells was calculated. Quantification of intratumoral microvessel density and apoptosis was performed by a blind observer to eliminate subjectivity of the analysis.

Results

Combination Therapy of TM and Doxorubicin Enhances Apoptosis *in Vitro*.

Apoptosis was determined by flow cytometry using FITC-Annexin V. As shown in Fig. 1A, apoptosis was not observed in these cells after TM (1–100 nM) treatment. A dose-dependent induction of apoptosis was observed with doxorubicin ranging from 9.9 ± 2.9% for 0.1 μM doxorubicin to 21.5 ± 2.0% for 2.5 μM doxorubicin. Doxorubicin (0.1 μM for 72 h) induced 75 ± 3.4% apoptosis in MDA-MB435 cells and 60 ± 2.1% apoptosis in MDA-MB231 cells. This observation indicates that SUM149 cells are relatively resistant to doxorubicin-induced apoptosis when compared with other commonly used breast carcinoma cell lines. In SUM149 cells, the combination therapy of TM and doxorubicin was more effective at inducing apoptosis than either compound administered alone; 33.8 ± 4.6%, 57.5 ± 5.2%, or 83.7 ± 1.0% apoptosis was observed in cells treated with TM and 0.1, 0.5, or 2.5 μM doxorubicin, respectively. Using ordinary least-squares regression framework to model these data, we found that this combination therapy resulted in a significant, greater-than-additive increase in apoptosis (P < 0.005; n = 3). Consistent with our apoptosis data, the clonogenic survival of cells treated with TM was similar to control (Fig. 1B). Doxorubicin induced a dose-dependent decrease in clonogenic survival, ranging from 118 ± 5 clones for 0.1 μM doxorubicin to 63 ± 8 clones for 2.5 μM doxorubicin. Importantly, the combination therapy was significantly more cytotoxic and resulted in fewer clones than single-agent doxorubicin therapy (P < 0.003; n = 3).

Combination Therapy of TM and Doxorubicin Suppresses Tumor Growth and Enhances Apoptosis *in Vivo*.

Female athymic nude mice were transplanted with SUM149 cells (1 × 10⁶), and palpable tumors were allowed to develop without treatment. At 28 days postimplantation, mice with established tumors of approximately 0.5 cm³ were randomly assigned to four protocols and treated with control (gavaged with water daily and i.v. injection with PBS weekly), TM (1.25 mg/day loading dose for 3 days followed by 0.7 mg/day maintenance dose for the remainder of protocol) by oral gavage, or doxorubicin (5 mg/kg/week) by i.v. injection or cotreated with TM (1.25 mg/day loading dose for 3 days followed by 0.7 mg/day maintenance dose for the remainder of protocol) and doxorubicin (5 mg/kg/week). Although the doubling time of control SUM149 tumors appears to be around 19 days, the experiment was terminated at 28 days posttreatment due to general health concerns because the size of the mammary tumors was bulky enough to impede mice from the control group from eating and drinking. Mice treated with TM as a single agent or in combination with doxorubicin were rendered copper deficient (ceruloplasmin
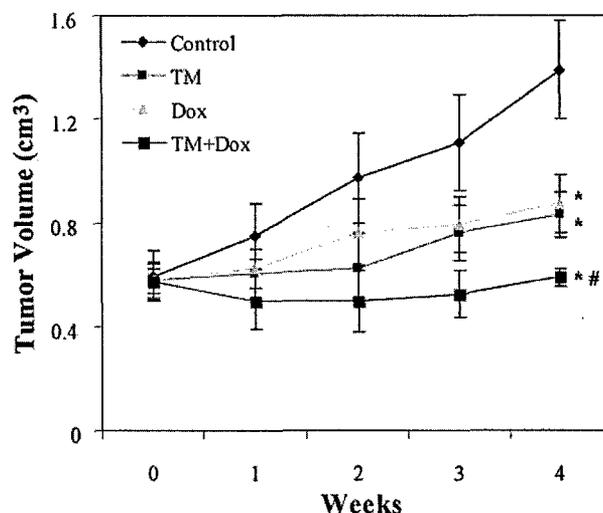

Fig. 2. Combination therapy of TM and doxorubicin inhibits tumor growth in SUM149 xenografts. SUM149 cells (1 × 10⁶) were orthotopically injected in the upper left mammary fat pad of 10-week-old athymic female mice. At 28 days after implantation, mice with established tumors of approximately 0.5 cm³ were randomly assigned to four protocols: control (gavaged with water daily and i.v. injection with PBS weekly); TM (1.25 mg/day loading dose for 3 days followed by 0.7 mg/day maintenance dose for the remainder of protocol) by oral gavage; doxorubicin (5 mg/kg/week) by i.v. injection; or cotreatment with TM (1.25 mg/day loading dose for 3 days followed by 0.7 mg/day maintenance dose for the remainder of protocol) and doxorubicin (5 mg/kg/week). Tumor volume was calculated as (length × width²)/2 and presented as mean ± SE. *, P < 0.05 *versus* control group; #, P < 0.03 *versus* TM- or doxorubicin-treated group; n = 6/treatment group.

levels < 25 ± 5% of control) after 1 week of therapy and remained so for the rest of the protocol. As shown in Fig. 2, therapy with TM or doxorubicin alone significantly inhibited tumor growth in comparison with control treatment (P < 0.05; n = 6). More importantly, mice treated with the combination of TM and doxorubicin had complete tumor stabilization without an apparent increase in toxicity as assessed by general health, weight, and behavior (P < 0.008 compared with control; P < 0.03 compared with TM or doxorubicin; n = 6).

Immunohistochemical analyses of the resected tumors revealed that intratumoral apoptosis was significantly higher than control in all treatment protocols (P < 0.01; 50% increase in the TM-treated group, 110% increase in the doxorubicin-treated group, and 220% increase in the combination-treated group). Moreover, tumor cell apoptosis was significantly higher in the combination therapy group than in either single-agent group of TM or doxorubicin (P < 0.01). As expected, tumors from the control group were highly vascularized, with a mean vessel count of 33 ± 4 (mean ± SE) per high-power field. In contrast, the smaller tumors resected from TM-treated (19 ± 2; P < 0.01), doxorubicin-treated (23 ± 3; P < 0.05), or TM and doxorubicin-treated (15 ± 2; P < 0.01) mice were significantly less vascularized per high-power field. The difference in microvessel density among these three treatment groups did not reach statistical significance (Fig. 3). Taken together, our data indicate that the combination therapy of TM and doxorubicin is more effective
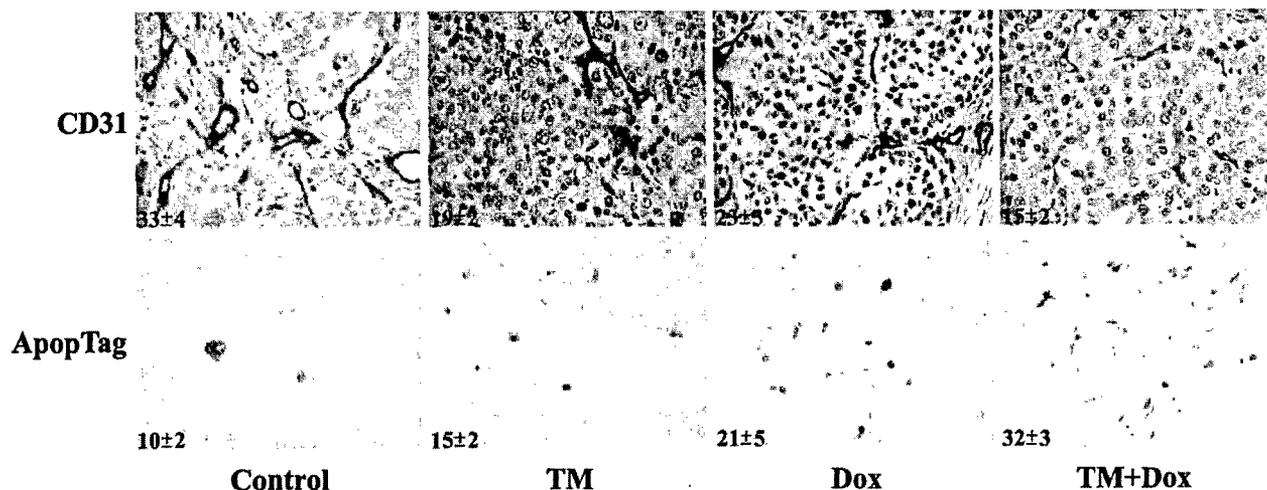
Fig. 3. Immunohistochemical analyses of SUM149 xenografts. Mammary tumors from control, TM-treated, doxorubicin-treated, and TM and doxorubicin combination-treated mice were resected and processed for immunohistochemical analysis. Intratumoral blood vessels were visualized using a CD31 antibody, and intratumoral cell apoptosis was visualized using the ApopTag kit. Mean vessel count/high-power field (×400) and mean number of apoptotic cells/500 total cells in a high-power field (×400) were calculated and presented as mean ± SE.

at suppressing tumor growth due to an increase in intratumoral apoptosis.

Discussion

The SUM149 inflammatory breast carcinoma cell line was derived from a primary tumor nodule in an inflammatory breast cancer patient that was refractory to conventional chemotherapy. Increased levels of NF-κB subunits, including p50, p52, and RelA, were found in SUM149 cells in comparison with immortalized HME cells (data not shown). Moreover, intrinsic NF-κB activity in SUM149 cells was about 2.5-fold higher than that in HME cells (11). Because constitutive activation of NF-κB is linked to resistance to several therapeutic modalities, we surmised that SUM149 cells may be refractory to conventional chemotherapy, consistent with the anthracycline resistance exhibited by the parental tumor in the patient. SUM149 cells were found to be resistant to doxorubicin (0.1 μM for 72 h)-induced apoptosis with about 90% cell survival. Under the same conditions, <40% of MDA-MB231 and <25% of MDA-MB435 breast carcinoma cells were viable. These results indicate that SUM149 cells are inherently extremely resistant to doxorubicin and thus an excellent system in which to examine the efficacy of combination therapies aimed at decreasing resistance.

Several groups demonstrated that inhibition of NF-κB activity sensitizes carcinoma cells with elevated levels of NF-κB to ionizing radiation and chemotherapeutic drugs (16, 17). Adenoviral delivery of dominant-negative IκBα sensitized chemoresistant tumors to the chemotherapeutic drug CPT-11 (18). With resistant lymphoid and leukemic cell lines, suppression of NF-κB resulted in an increased sensitivity to induction of apoptosis by doxorubicin (8). These studies provide direct evidence that inhibition of NF-κB is effective *in vitro* in enhancing therapeutic efficacy against carcinoma cells with elevated NF-κB activity. Our laboratory reported that copper deficiency induced by TM has antiangiogenic

properties, in part, through blockade of the NF-κB signaling cascade (11). In SUM149 cells, TM treatment resulted in a significant decrease in NF-κB activation and expression (11). This observation led us to examine whether TM can enhance the efficacy of conventional chemotherapy against SUM149 cells. Our data demonstrate that the combination therapy of TM and doxorubicin was significantly more effective than either agent alone at inducing apoptosis *in vitro*. Using an alternate treatment regimen, cells pretreated with TM (1 nM for 72 h) were about 3-fold more sensitive to doxorubicin-induced apoptosis (data not shown). These results indicate that TM, under cotreatment or pretreatment conditions, enhances SUM149 cells to doxorubicin-induced apoptosis, consistent with TM's known suppression of NF-κB activity.

In our xenograft animal study, single-agent therapy with TM resulted in significantly smaller tumors with a decrease in mean intratumoral vessel density and an increase in intratumoral apoptosis. Surprisingly, *in vivo*, tumor growth was inhibited, and intratumoral apoptosis was increased with doxorubicin treatment. We anticipated that the SUM149 xenografts would be refractory to doxorubicin, based on our *in vitro* data demonstrating the resistance of these cells to doxorubicin-induced apoptosis. Interestingly, doxorubicin lowered mean vessel density to the same extent as TM (about 40% inhibition), indicating that the dose and scheduling of doxorubicin used in this study have a significant antiangiogenic effect. From this result, we suggest that the intratumoral apoptosis observed with doxorubicin is not a direct effect of cytotoxicity but possibly an indirect result of inhibiting tumor angiogenesis, through either inhibition of endothelial cell proliferation or suppression of angiogenic mediators produced by tumor cells. Importantly, the growth of well-established bulky tumors was completely stabilized with the combination therapy of TM and doxorubicin, likely due to the fact that intratumoral apoptosis from the combination treatment group was significantly higher than that

seen with either TM or doxorubicin treatment alone. In a separate study, nuclear proteins extracted from tumors in TM-treated mice showed a significant decrease in NF-κB binding activity.[4] In light of these findings, we postulate that in the combination therapy regimen, TM is sensitizing the established SUM149 tumors by suppressing NF-κB activation, thereby reverting these tumor cells to a phenotype responsive to doxorubicin-induced apoptosis.

Accumulating evidence indicates a therapeutic benefit of combining antiangiogenic compounds with conventional chemotherapy. Antiangiogenic compounds were reported to potentiate antineoplastic therapies against primary and metastatic disease, presumably through increased delivery of antineoplastic agents into the tumor mass (19, 20). It is speculated that an overabundance of endothelial cells in established tumors contributes to the formation of abnormal dilated leaky vessels within the tumor mass (21, 22). Apoptosis of tumor endothelial cells, through targeted direct or indirect antiangiogenic therapies, results in a decrease of immature leaky tumor vessels (23, 24). It is further suggested that pruning of these abnormal vessels leads to a more "normalized" tumor vasculature, thereby allowing for more efficient delivery of therapeutic compounds (25). In keeping with this line of reasoning, we hypothesize that TM, a global inhibitor of proangiogenic mediators including vascular endothelial growth factor, may be normalizing the tumor vasculature, resulting in increased delivery of doxorubicin. It could be argued that the enhanced efficacy observed with the combination therapy is just due to a higher concentration of doxorubicin in the tumor mass. However, if this were the case, then the intratumoral apoptosis observed with single-agent doxorubicin would be similar to the combination therapy. Single-agent doxorubicin resulted in a decrease in intratumoral microvessel density, and therefore, by the same argument, may be remodeling the tumor vasculature to allow for increased delivery of doxorubicin. Beyond the scope of our work, additional experiments such as measurements of intratumoral doxorubicin levels at several time points would be necessary to address this possibility. Nevertheless, the fact that treatment with doxorubicin and TM was significantly more effective at inducing apoptosis than single-agent doxorubicin suggests that TM must have an additional direct effect on the tumor cells, namely, sensitization of these cells to doxorubicin-induced apoptosis.

In conclusion, TM was shown to enhance the efficacy of doxorubicin in mammary carcinoma cells. This study provides strong support for the evaluation of TM in combination with anthracyclines, especially doxorubicin, in future clinical trials of locally advanced breast carcinoma. One suitable clinical end point suggested by this work would be the rate of pathological complete response after multiple cycles of combination therapy with TM and anthracyclines.

---

[4] Q. Pan, L. W. Bao, and S. D. Merajver, unpublished data.

References

1. George, S. L., and Desu, M. M. Planning the size and duration of a clinical trial studying the time to some critical event. J. Chronic. Dis., *27:* 15–24, 1974.

2. Barth, T. F., Dohner, H., Werner, C. A., Stilgenbauer, S., Schlotter, M., Pawlita, M., Lichter, P., Moller, P., and Bentz, M. Characteristic pattern of chromosomal gains and losses in primary large B-cell lymphomas of the gastrointestinal tract. Blood, *91:* 4321–4330, 1998.

3. Mathew, S., Murty, V. V., Dalla-Favera, R., and Chaganti, R. S. Chromosomal localization of genes encoding the transcription factors, c-rel, NF-κBp50, NF-κBp65, and lyt-10 by fluorescence in situ hybridization. Oncogene, *8:* 191–193, 1993.

4. Motokura, T., and Arnold, A. PRAD1/cyclin D1 proto-oncogene: genomic organization, 5′ DNA sequence, and sequence of a tumor-specific rearrangement breakpoint. Genes Chromosomes Cancer, *7:* 89–95, 1993.

5. Nakshatri, H., Bhat-Nakshatri, P., Martin, D. A., Goulet, R. J., Jr., and Sledge, G. W., Jr. Constitutive activation of NF-κB during progression of breast cancer to hormone-independent growth. Mol. Cell. Biol., *17:* 3629–3639, 1997.

6. Sovak, M. A., Bellas, R. E., Kim, D. W., Zanieski, G. J., Rogers, A. E., Traish, A. M., and Sonenshein, G. E. Aberrant nuclear factor-κB/Rel expression and the pathogenesis of breast cancer. J. Clin. Investig., *100:* 2952–2960, 1997.

7. Paillard, F. Induction of apoptosis with I-κB, the inhibitor of NF-κB. Hum. Gene Ther., *10:* 1–3, 1999.

8. Jeremias, I., Kupatt, C., Baumann, B., Herr, I., Wirth, T., and Debatin, K. M. Inhibition of nuclear factor κB activation attenuates apoptosis resistance in lymphoid cells. Blood, *91:* 4624–4631, 1998.

9. Giri, D. K., and Aggarwal, B. B. Constitutive activation of NF-κB causes resistance to apoptosis in human cutaneous T cell lymphoma HuT-78 cells. Autocrine role of tumor necrosis factor and reactive oxygen intermediates. J. Biol. Chem., *273:* 14008–14014, 1998.

10. Brewer, G. J., Dick, R. D., Grover, D. K., LeClaire, V., Tseng, M., Wicha, M., Pienta, K., Redman, B. G., Jahan, T., Sondak, V. K., Strawderman, M., LeCarpentier, G., and Merajver, S. D. Treatment of metastatic cancer with tetrathiomolybdate, an anticopper, antiangiogenic agent: Phase I study. Clin. Cancer Res., *6:* 1–10, 2000.

11. Pan, Q., Kleer, C. G., van Golen, K. L., Irani, J., Bottema, K. M., Bias, C., De Carvalho, M., Mesri, E. A., Robins, D. M., Dick, R. D., Brewer, G. J., and Merajver, S. D. Copper deficiency induced by tetrathiomolybdate suppresses tumor growth and angiogenesis. Cancer Res., *62:* 4854–4859, 2002.

12. Khan, M. K., Miller, M. W., Taylor, J., Gill, N. K., Dick, R. D., van Golen, K. L., Brewer, G. J., and Merajver, S. D. Radiotherapy and anti-angiogenic TM in lung cancer. Neoplasia, *4:* 164–170, 2002.

13. Cox, C., Teknos, T. N., Barrios, M., Brewer, G. J., Dick, R. D., and Merajver, S. D. The role of copper suppression as an antiangiogenic strategy in head and neck squamous cell carcinoma. Laryngoscope, *111:* 696–701, 2001.

14. Ignatoski, K. M., and Ethier, S. P. Constitutive activation of pp125fak in newly isolated human breast cancer cell lines. Breast Cancer Res. Treat., *54:* 173–182, 1999.

15. Weidner, N. Intratumor microvessel density as a prognostic factor in cancer. Am. J. Pathol., *147:* 9–19, 1995.

16. Liu, Z. G., Hsu, H., Goeddel, D. V., and Karin, M. Dissection of TNF receptor 1 effector functions: JNK activation is not linked to apoptosis while NF-κB activation prevents cell death. Cell, *87:* 565–576, 1996.

17. Wang, C. Y., Mayo, M. W., and Baldwin, A. S., Jr. TNF- and cancer therapy-induced apoptosis: potentiation by inhibition of NF-κB. Science (Wash. DC), *274:* 784–787, 1996.

18. Wang, C. Y., Cusack, J. C., Jr., Liu, R., and Baldwin, A. S., Jr. Control of inducible chemoresistance: enhanced anti-tumor therapy through increased apoptosis by inhibition of NF-κB. Nat. Med., *5:* 412–417, 1999.

19. Teicher, B. A., Sotomayor, E. A., and Huang, Z. D. Antiangiogenic agents potentiate cytotoxic cancer therapies against primary and metastatic disease. Cancer Res., *52:* 6702–6704, 1992.

20. Kakeji, Y., and Teicher, B. A. Preclinical studies of the combination of angiogenic inhibitors with cytotoxic agents. Invest. New Drugs, *15:* 39–48, 1997.

21. Baish, J. W., and Jain, R. K. Fractals and cancer. Cancer Res., *60:* 3683–3688, 2000.

22. Gazit, Y., Baish, J. W., Safabakhsh, N., Leunig, M., Baxter, L. T., and Jain, R. K. Fractal characteristics of tumor vascular architecture during tumor growth and regression. Microcirculation, *4:* 395–402, 1997.

23. Yuan, F., Chen, Y., Dellian, M., Safabakhsh, N., Ferrara, N., and Jain, R. K. Time-dependent vascular regression and permeability changes in established human tumor xenografts induced by an anti-vascular endothelial growth factor/vascular permeability factor antibody. Proc. Natl. Acad. Sci. USA, *93:* 14765–14770, 1996.

24. Jain, R. K., Safabakhsh, N., Sckell, A., Chen, Y., Jiang, P., Benjamin, L., Yuan, F., and Keshet, E. Endothelial cell death, angiogenesis, and microvascular function after castration in an androgen-dependent tumor: role of vascular endothelial growth factor. Proc. Natl. Acad. Sci. USA, *95:* 10820–10825, 1998.

25. Jain, R. K. Normalizing tumor vasculature with anti-angiogenic therapy: a new paradigm for combination therapy. Nat. Med., *7:* 987–989, 2001.

Tetrathiomolybdate Inhibits Angiogenesis and Metastasis Through Suppression of the NFκB Signaling Cascade

Quintin Pan, Li Wei Bao, and Sofia D. Merajver

Department of Internal Medicine, Division of Hematology and Oncology and Comprehensive Cancer Center, University of Michigan Medical School, Ann Arbor, MI

Abstract

Tetrathiomolybdate (TM), a specific copper chelator, has been shown to be a potent antiangiogenic and antimetastatic compound possibly through suppression of the NFκB signaling cascade. To further delineate the molecular mechanism of the anticancer effect of TM, we investigated whether TM has antineoplastic activity in the setting of genetic NFκB inhibition. In this study, SUM149 inflammatory breast carcinoma cells were transfected with a dominant-negative IκBα (S32AS36A) expression vector. Similar to TM-treated SUM149 cells, SUM149-IκBαMut clones secreted lower amounts of proangiogenic mediators, vascular endothelial growth factor, interleukin-1α, and interleukin-8 and exhibited a less invasive and motile phenotype. The reduction in the angiogenic and metastatic potential of SUM149-IκBαMut clones was not further affected by TM in vitro. SUM149-IκBαMut xenografts grew substantially slower and had less lung metastasis than SUM149 and SUM149-empty vector xenografts. The growth and metastatic potential of SUM149 and SUM149-empty tumors was significantly inhibited with systemic TM treatment, whereas TM had no further antitumor effect on the SUM149-IκBαMut tumors. Additionally, nuclear proteins isolated from TM-treated SUM149 tumors had lower NFκB binding activity, while AP1 and SP1 binding activities were unchanged. Taken together, these results strongly support that suppression of NFκB is the major mechanism used by TM to inhibit angiogenesis and metastasis.

Introduction

Evidence has accumulated in the past decade that establishes an incontrovertible link between uncontrolled NFκB activity and oncogenesis. Numerous reports have characterized various types of solid tumors with deregulated NFκB activity as a result of constitutive activation of the NFκB signaling pathway or inactivating mutations of IκB protein members (1–5). Chromosomal aberrations spanning regions containing RelA, c-Rel, p50, and p52 genes were found in many hematopoietic and solid tumors (1). Amplification of RelA was reported in squamous carcinomas of the head and neck, breast, and gastric cancers (2, 3). Additionally, overexpression of p50 and p52 was observed in colon, prostate, and breast carcinomas (6, 7). As a whole, these reports indicate that constitutive activation of NFκB appears to be an event that frequently occurs during malignant transformation of cells.

NFκB has been shown to regulate a whole cadre of genes important for angiogenesis, invasion, and metastasis (5, 8–12). Blockade of NFκB activity suppressed vascular endothelial growth factor (VEGF) and interleukin (IL)-8 expression, resulting in a decrease in tumor angiogenesis in ovarian and prostate carcinoma cells (13, 14). Additionally, NFκB inhibition was reported to suppress invasion and metastasis of highly metastatic PC-3 prostate carcinoma cells (14). PS-341 (VELCADE), a proteasome inhibitor that blocks NFκB activation through the prevention of IκB degradation, was found to suppress tumor growth that correlated with a decrease in intratumoral microvessel density (15). 2-Methoxyestradiol, an endogenous estrogenic metabolite with antiangiogenic properties, inhibited NFκB activity in DAOY medulloblastoma cells (16). Our laboratory demonstrated that tetrathiomolybdate (TM) inhibits tumor growth and angiogenesis in SUM149 inflammatory breast carcinoma and squamous cell carcinoma V11/SF xenografts (17, 18). *In vitro*, TM suppressed NFκB activity and decreased the amount of known NFκB-dependent proangiogenic mediators, VEGF, IL-1, IL-6, and IL-8 released by SUM149 cells, indicating that the degree of inhibition of these NFκB-dependent factors was sufficient to drastically affect tumor growth (17). Further, TM was shown to potently block lung metastases in nude mice implanted with DU145 prostate carcinoma cells (19). These results suggest that a major mechanism of the anticancer effect of TM is suppression of NFκB, leading to a global inhibition of NFκB-mediated transcription of proangiogenic and prometastatic genes. However, it is not known whether other mechanisms contribute to the anticancer effect of TM. To discern this question, we set out to independently inhibit NFκB activity in SUM149 inflammatory breast carcinoma cells and assess the effect of adding TM to this intervention.

Results and Discussion

Inflammatory breast cancer is highly angiogenic and invasive, giving rise to profusely vascularized tumors at the

primary and distant metastatic sites (20). It is thus an excellent, stringent model to test potential antiangiogenic strategies. Previous reports from our laboratory have demonstrated that SUM149 cells produce high levels of proangiogenic mediators, VEGF, FGF2, IL-6, and IL-8 and exhibit an extremely invasive and motile phenotype (21, 22). Because NFκB activation has been shown to be an inducer of angiogenesis and metastasis and TM, an inhibitor of NFκB, was reported to be antiangiogenic and antimetastatic, we investigated if SUM149 cells are dependent on constitutive NFκB activation for its highly angiogenic and metastatic phenotype. To this end, SUM149 cells were stably transfected with an IκBα mutant expression vector, which encodes a dominant negative IκBα (S32AS36A). SUM149-IκBαMut-transfected cells were selected in G418-containing medium, and three positive clones (clones 1–3) were expanded and maintained in the selection medium. In Fig. 1A, reverse transcription-PCR analysis showed higher expression of IκBα mRNA in clones 2 and 3 in comparison with untransfected or empty vector-transfected SUM149 (SUM149-empty) cells. Similarly, protein levels of IκBα were significantly increased in clones 2 and 3 (Fig. 1B).

To characterize the effect of NFκB suppression in SUM149 cells, conditioned media from SUM149-IκBαMut clones were collected and measured for VEGF, IL-1α, and IL-8 by ELISA. Consistent with our previous report, secretion of these
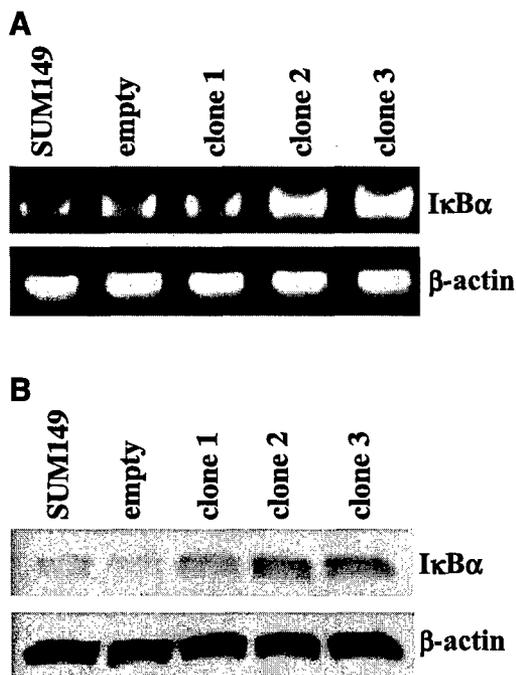

FIGURE 1. Reverse transcription-PCR and Western blot of IκBα in SUM149 and SUM149-IκBαMut clones. **A.** mRNA expression of IκBα. Quantitative reverse transcription-PCR was performed on mRNA extracts from SUM149, SUM149-empty vector, and SUM149-IκBαMut clones using specific primers for the IκBα and β-actin gene. **B.** Protein levels of IκBα. Western blot analysis was performed on whole-cell lysates from SUM149, SUM149-empty vector, and SUM149-IκBαMut clones using specific antibodies for the IκBα and β-actin protein. This figure is representative of four independent experiments.

proangiogenic mediators by SUM149 cells was significantly inhibited following TM treatment (10 nM for 72 h). Similarly, SUM149-IκBαMut clones 2 and 3 secreted lower amounts of these proangiogenic mediators in comparison with untransfected or empty vector-transfected SUM149 cells ($P < 0.05$) (Fig. 2A). We focused our attention on VEGF, IL-1α, and IL-8 due to their known dependence on NFκB and by no means a complete list of genes regulated by TM. Because induction of tumor angiogenesis is due to a change in the proangiogenic/antiangiogenic balance, it is certainly likely that TM is able to modulate the expression and levels of other proangiogenic and antiangiogenic mediators. Work with cDNA microarray and proteomics is ongoing in our laboratory to address this question in a comprehensive manner. TM (10 nM for 48 h) blocked invasion by $50.8 \pm 1.6\%$ ($P < 0.04$) and motility by $21 \pm 2.7\%$ ($P < 0.005$) in SUM149 cells. Likewise, SUM149-IκBαMut clones are less invasive ($40.5 \pm 2.2\%$ and $59.5 \pm 6.3\%$ inhibition for clones 2 and 3, respectively) and motile ($22.8 \pm 1.8\%$ and $35.9 \pm 4.1\%$ inhibition for clones 2 and 3, respectively) than wild-type SUM149 cells. TM treatment of SUM149-IκBαMut clones resulted in no additional effect on inhibiting invasion, metastasis, and amount of proangiogenic mediators. These results demonstrate that NFκB plays a major role in establishing the angiogenic and metastatic phenotype of inflammatory breast cancer cells. Moreover, because the change in phenotype observed for TM-treated SUM149 cells is similar to untreated SUM149-IκBαMut clones and TM did not change the phenotype of SUM149-IκBαMut clones, there is evidence that inhibition of tumor angiogenesis and metastasis by TM is a direct consequence of the ability of TM to suppress NFκB activation.

To determine if the antiangiogenic and antimetastatic actions of TM are a result of inhibiting NFκB activation in vivo, SUM149, SUM149-empty, SUM149-IκBαMut clone 2, or SUM149-IκBαMut clone 3 cells (1×10^6) were orthotopically transplanted into the mammary fat pads of 10-week-old female athymic nude mice. Mice were gavaged with water (control) or TM (1.25 mg/day for the first 3 days and 0.7 mg/day for the remainder of the protocol) starting on the day of xenograft transplantation. Ceruloplasmin was followed weekly and used as a surrogate marker for serum copper status. After 1 week of treatment, ceruloplasmin levels of TM-treated mice were maintained at less than 25% of baseline for the remainder of the protocol. Consistent with our previous report, TM significantly inhibited the tumor growth of SUM149 xenografts ($74.6 \pm 5.0\%$ inhibition; $P < 0.001$). TM-treated SUM149 tumor-bearing mice had a lower incidence of lung metastasis in comparison with untreated SUM149 tumor-bearing mice (1/6 vs. 6/6 mice). The size of SUM149-empty tumors was smaller by $69.4 \pm 1.1\%$ ($P < 0.001$), and incidence of lung metastasis was lower (0/6 vs. 5/6 mice) as a result of systemic TM therapy (Fig. 3A). SUM149-IκBαMut clones 2 and 3 tumors were significantly less bulky ($P < 0.001$, $n = 6$) and less metastatic (only 0/6 and 1/6 mice had lung metastasis for clones 2 and 3, respectively) in contrast to the SUM149 and SUM149-empty tumors. Importantly, tumor growth and incidence of lung metastasis of SUM149-IκBαMut clones 2 and 3 bearing mice was unchanged with TM treatment.
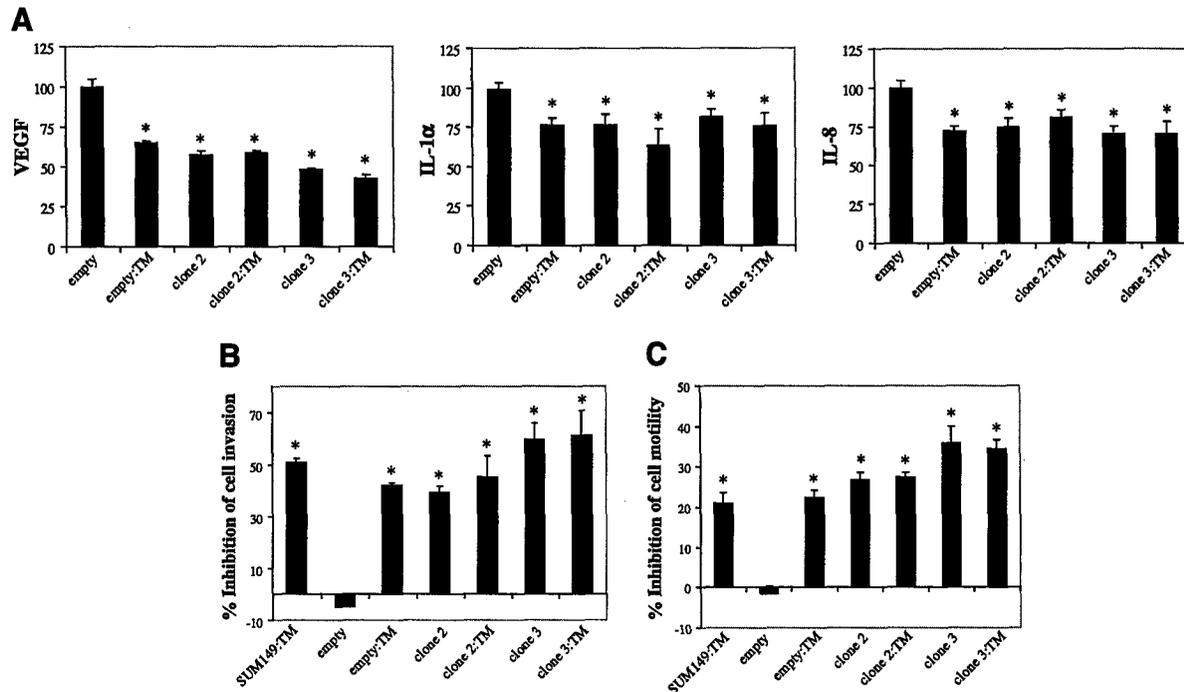
FIGURE 2. Phenotype characterization of SUM149 and SUM149-IκBαMut clones. **A.** Proangiogenic mediators. SUM149, SUM149-empty vector, SUM149-IκBαMut clone 2, or SUM149-IκBαMut clone 3 cells were plated and treated with vehicle or 10-nM TM for 72 h. Conditioned media were collected and measured for VEGF, IL-1α, and IL-8 by ELISA. *P < 0.05 vs. untreated SUM149-empty vector. **B.** Cell invasion. Cells were pretreated with or without 10-nM TM for 48 h, harvested, and resuspended in serum-free medium. An aliquot (1 × 10^5 cells) of the prepared cell suspension was added into the chamber and incubated for 48 h at 37°C in a 10% CO_2 tissue culture incubator. Noninvading cells were gently removed from the interior of the inserts with a cotton-tipped swab. Invasive cells were stained and quantified by colorimetric reading at 560 nm. *P < 0.04 vs. untreated SUM149 wild-type or untreated SUM149-empty vector. **C.** Cell motility. Cells were pretreated with or without 10-nM TM for 48 h, harvested, suspended in serum-free medium, and plated on top of a field of microscopic fluorescent beads. After a 48-h incubation period, cells were fixed, and areas of clearing in the fluorescent bead field corresponding to phagokinetic cell tracks were quantified using NIH ScionImager. *P < 0.005 vs. untreated SUM149 wild-type or SUM149-empty vector.

To directly determine the effect of TM on NFκB activity of cancer cells in the tumor mass, mammary tumors were resected and nuclear proteins were isolated for electrophoretic mobility shift assay (Fig. 3C). Constitutive intratumoral NFκB binding was observed for untreated SUM149 and SUM149-empty xenografts. Systemic TM therapy resulted in lower NFκB binding in SUM149 and SUM149-empty tumors. As expected, expression of dominant-negative IκBα significantly inhibited NFκB activity of SUM149-IκBαMut tumors. To determine the specificity of nuclear protein binding to κB consensus sequence, competition experiments were performed with unlabeled κB, AP1, and SP1 (Fig. 3D). Nuclear protein binding to κB was specific as excess (100-fold) unlabeled κB completely displaced binding, whereas κB binding was unchanged with the addition of excess (100-fold) unlabeled AP1 or SP1. Moreover, AP1 and SP1 binding was unaffected with TM therapy, suggesting that TM is specifically targeting NFκB activity of cancer cells within the tumor mass. The observation that these carcinoma cells remained responsive to TM even after 7 weeks of continuous daily therapy suggests that the incidence of resistance to TM may be lower than conventional cytotoxic chemotherapeutic agents. This is exciting from a clinical perspective, as it appears that TM may prove to be more resilient and be efficacious against solid tumors for a prolonged period. These *in vivo* results are

consistent with our *in vitro* observations and further support the notion that inhibition of NFκB in carcinoma cells is a major component of the antiangiogenic and antimetastatic actions of TM.

Tumor angiogenesis is a dynamic and complex process that involves multiple proangiogenic mediators. Recent reports have demonstrated that a number of proangiogenic mediators are up-regulated in numerous solid tumors, including breast, ovarian, and prostate carcinomas, and sarcomas and a critical event in tumor progression (13, 14, 22, 23). Because several proangiogenic mediators are involved in the stimulation of tumor angiogenesis, it is critical to recognize that blockade of one proangiogenic mediator alone may not be sufficient to inhibit angiogenesis to an extent required for clinical response. Recent failures of late-stage cancer trials for VEGF-KDR antagonists, SU-5416 and Avastin, lend further credence for the need to develop broad-spectrum antiangiogenic agents that can target multiple proangiogenic mediators. In a phase 2 clinical trial for advance renal cell carcinoma, patients rendered copper deficient by TM significantly had lower amounts of proangiogenic mediators, VEGF, FGF2, IL-6, and IL-8 in circulation than prior to therapy (24). It appears that TM is capable of attacking multiple proangiogenic targets and may prove to be more efficacious than single-target therapy for the treatment of solid tumors in future phase 3 clinical trials.
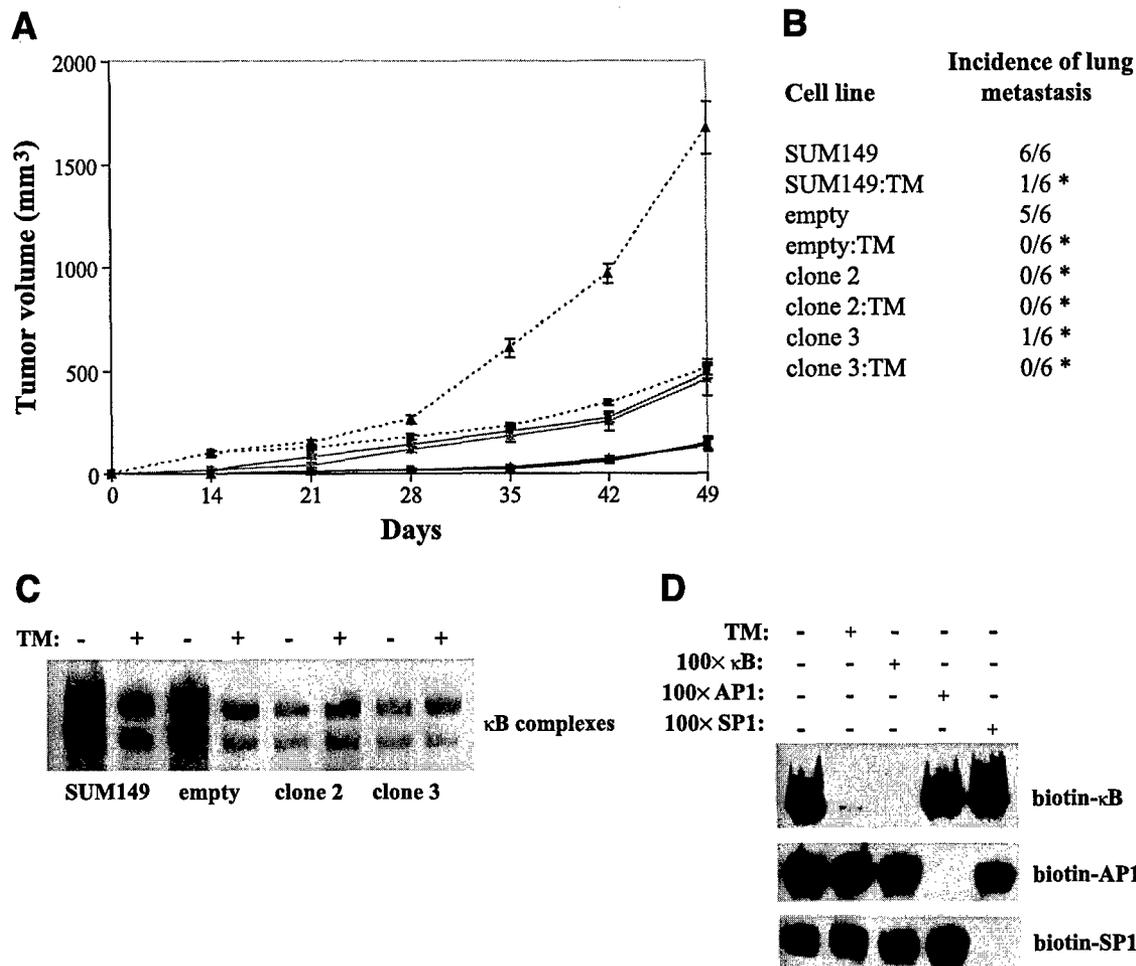
A

B

Cell line	Incidence of lung metastasis
SUM149	6/6
SUM149:TM	1/6 *
empty	5/6
empty:TM	0/6 *
clone 2	0/6 *
clone 2:TM	0/6 *
clone 3	1/6 *
clone 3:TM	0/6 *

C

TM: - + - + - + - +

κB complexes

SUM149   empty   clone 2   clone 3

D

TM:	-	+	-	-	-
100× κB:	-	-	+	-	-
100× AP1:	-	-	-	+	-
100× SP1:	-	-	-	-	+

biotin-κB

biotin-AP1

biotin-SP1

FIGURE 3. Effects of systemic TM therapy on SUM149 and SUM149-IκBαMut xenografts in nude mice. **A.** Tumor growth. SUM149, SUM149-empty vector, SUM149-IκBαMut clone 2, or SUM149-IκBαMut clone 3 cells were orthotopically injected into the upper left mammary fat pad of 10-week-old female athymic nude mice. At day of tumor implantation, mice were randomly assigned and gavaged with water (control) or TM (1.25 mg/day for first 3 days and 0.7 mg/day for the remainder of the protocol). Tumor growth was measured weekly using a microcaliper, and tumor volume was calculated using the formula: (length × width²) / 2. ---▲---, empty; ---■---, empty:TM; —▲—, clone 2; —■—, clone 2:TM; —▲—, clone 3; —■—, clone 3:TM. **B.** Incidence of lung metastasis. At the end of the experimental protocol, lungs were removed, and gross lung metastasis was counted on the lung surface under 100× magnification using a dissecting microscope. *$P < 0.02$ vs. untreated SUM149 wild-type or SUM149-empty vector. **C.** Intratumoral NFκB binding activity. At the end of the experimental protocol, primary mammary tumors were resected, and nuclear proteins were isolated. Electrophoretic mobility shift assay was performed with biotin-labeled κB consensus sequence. This is representative of four independent experiments. **D.** Competition electrophoretic mobility shift assay with NFκB, AP1, and SP1. Electrophoretic mobility shift assay was performed with nuclear proteins isolated from control and TM-treated SUM149 wild-type tumors and incubated with biotin-labeled κB consensus sequence, AP1 consensus sequence, or SP1 consensus sequence in the absence or presence of 100× unlabeled κB, AP1, or SP1. This is representative of four independent experiments.

As a whole, these results solidly demonstrate that the major component of the antiangiogenic and antimetastatic actions of TM are due to the direct effect of TM on inhibiting NFκB activity of cancer cells, thus impairing these malignant cells from producing and releasing mediators required for angiogenesis and metastasis into the tumor microenvironment.

Materials and Methods
Cell Lines

The SUM149 inflammatory breast cancer cell line was developed from a primary inflammatory breast cancer tumor and grown in Ham's F-12 medium supplemented with 5% fetal bovine serum, 5-μg/ml insulin, and 1-μg/ml hydrocortisone.

Transfection With IκBαMut Expression Vector

SUM149 cells were transfected with pUSEamp-empty vector or pUSEamp-IκBαDN (S32AS36A) (Upstate Biotechnology, Inc., Lake Placid, NY) using FuGene 6 transfection reagent (Roche-Boehringer Mannheim, Mannheim, Germany). Stable transfectants were established by culturing the transfected cells in the described medium supplemented with 100-μg/ml G418 (Life Technologies, Inc., Carlsbad, CA) for 21 days. Expression of the transgene was determined by reverse transcription-PCR and Western blot analysis.

Messenger RNA Expression and Protein Levels of IκBαMut Clones

Total RNA was isolated from cells using Trizol reagent (Life

Technologies) according to the manufacturer's recommendations. One microgram of total RNA was converted to cDNA using an avian myeloblastosis virus reverse transcription system (Promega, Madison, WI). A 100-μg aliquot of the resulting cDNA was amplified by PCR with 25-ng IκBα or β-actin specific primers. PCR products were separated on a 1.2% agarose gel and imaged on an Alpha Image 950 documentation system (Alpha Innotech, San Leandro, CA). Densitometry of images was performed using NIH Image version 1.62.

Proteins were harvested from SUM149, SUM149-empty vector, and SUM149-IκBαMut clones 1–3 cells using radioimmunoprecipitation assay buffer (1× PBS, 1% NP40, 0.5% sodium deoxycholate, 0.1% SDS, 0.1-mg/ml phenylmethylsulfonyl fluoride, 1-mM sodium orthovanadate, and 0.3-mg/ml aprotinin; Sigma Chemical Co., St. Louis, MO). Proteins (20 μg) were mixed with Laemelli buffer, heat denatured for 3 min, separated by 10% SDS-PAGE, and transferred to polyvinylidene difluoride membrane. Nonspecific binding was blocked by overnight incubation with 2% BSA in Tris-buffered saline with 0.05% Tween 20 (Sigma). Immobilized proteins were probed using antibodies specific for IκBα and β-actin (Upstate Biotechnology) and visualized by enhanced chemiluminescence (Amersham, Piscataway, NJ).

Conditioned Medium From SUM149 Cells

SUM149 and SUM149-IκBαMut cells were plated at a density of 2×10^5 cells in 100-mm^2 dishes. Cells were treated with vehicle or 10-nM TM for 72 h. Conditioned medium was collected, centrifuged for 5 min at 2500 rpm, and divided into 1-ml aliquots. Quantikine human VEGF ELISA (R&D Systems, Inc., Minneapolis, MN) was used to measure protein levels of the 165 amino acid species of VEGF. ELISAs for IL-1α and IL-8 were performed by the University of Maryland Cytokine Core Laboratory (www.cytokinelab.com).

Cell Invasion and Motility Assay

Cell invasion was determined as described from the cell invasion assay kit (Chemicon International, Inc., Temecula, CA). Cells were pretreated with or without 10-nM TM for 48 h, harvested, and resuspended in serum-free medium. An aliquot (1×10^5 cells) of the prepared cell suspension was added into the chamber and incubated for 48 h at 37°C in a 10% CO_2 tissue culture incubator. Noninvading cells were gently removed from the interior of the inserts with a cotton-tipped swab. Invasive cells were stained and quantified by colorimetric reading at 560 nm. Random cell motility was determined as described from the motility assay kit (Cellomics, Pittsburgh, PA). Cells were pretreated with or without 10-nM TM for 48 h, harvested, suspended in serum-free medium, and plated on top of a field of microscopic fluorescent beads. After a 48-h incubation period, cells were fixed, and areas of clearing in the fluorescent bead field corresponding to phagokinetic cell tracks were quantified using NIH ScionImager.

Xenograft Model of Breast Cancer

Ten-week-old female athymic nude mice were orthotopically injected with SUM149 cells (1×10^6 cells) into the upper left mammary fat pad. Cells were trypsinized, washed, and resuspended in HBSS at a density of 1×10^6 cells/200 μl. Mice were anesthetized using 10-mg/ml ketamine, 1-mg/ml xylazine, and 0.01-mg/ml glycopyrrolate, and an incision below the thoracic left mammary fat pad was made. Using a 27-gauge needle, the cell suspension was injected into the exposed mammary fat pad and the wound was closed with a single wound clip.

Electrophoretic Mobility Shift Assay

Mammary tumors were resected and nuclear proteins were isolated using NE-PER nuclear protein extraction kit (Pierce Biotechnology, Rockford, IL). Electrophoretic mobility shift assay was performed as described using the LightShift Chemiluminescent EMSA kit (Pierce Biotechnology) with biotin-labeled κB consensus sequence, 5'-AGTTGAGG-GACTTTCCCAGGC-3', AP1 consensus sequence, 5'-CGCTTGATGAGTCAGCCCGGAA-3', or SP1 consensus sequence, 5'-ATTCGATCGGGGCGGGGCGAGC-3' in the absence or presence of 100× unlabeled κB, AP1, or SP1 oligonucleotide. Protein-DNA complexes were resolved on a high ionic strength 5% polyacrylamide gel containing 0.5× Tris-borate EDTA buffer.

References
1. Barth, T. F., Dohner, H., Werner, C. A., Stilgenbauer, S., Schlotter, M., Pawlita, M., Lichter, P., Moller, P., and Bentz, M. Characteristic pattern of chromosomal gains and losses in primary large B-cell lymphomas of the gastrointestinal tract. Blood, *91:* 4321–4330, 1998.

2. Mathew, S., Murty, V. V., Dalla-Favera, R., and Chaganti, R. S. Chromosomal localization of genes encoding the transcription factors, c-rel, NF-κBp50, NF-κBp65, and lyt-10 by fluorescence in situ hybridization. Oncogene, *8:* 191–193, 1993.

3. Motokura, T. and Arnold, A. PRAD1/cyclin D1 proto-oncogene: genomic organization, 5' DNA sequence, and sequence of a tumor-specific rearrangement breakpoint. Genes Chromosomes Cancer, *7:* 89–95, 1993.

4. Nakshatri, H., Bhat-Nakshatri, P., Martin, D. A., Goulet, R. J., Jr., and Sledge, G. W., Jr. Constitutive activation of NF-κB during progression of breast cancer to hormone-independent growth. Mol. Cell. Biol., *17:* 3629–3639, 1997.

5. Sovak, M. A., Bellas, R. E., Kim, D. W., Zanieski, G. J., Rogers, A. E., Traish, A. M., and Sonenshein, G. E. Aberrant nuclear factor-κB/Rel expression and the pathogenesis of breast cancer. J. Clin. Invest., *100:* 2952–2960, 1997.

6. Cogswell, P. C., Guttridge, D. C., Funkhouser, W. K., and Baldwin, A. S., Jr. Selective activation of NF-κB subunits in human breast cancer: potential roles for NF-κB2/p52 and for Bcl-3. Oncogene, *19:* 1123–1131, 2000.

7. Bours, V., Dejardin, E., Goujon-Letawe, F., Merville, M. P., and Castronovo, V. The NF-κB transcription factor and cancer: high expression of NF-κ. Biochem. Pharmacol., *47:* 145–149, 1994.

8. Libermann, T. A. and Baltimore, D. Activation of interleukin-6 gene expression through the NF-κB transcription factor. Mol. Cell. Biol., *10:* 2327–2334, 1990.

9. Kunsch, C. and Rosen, C. A. NF-κB subunit-specific regulation of the interleukin-8 promoter. Mol. Cell. Biol., *13:* 6137–6146, 1993.

10. van de Stolpe, A., Caldenhoven, E., Stade, B. G., Koenderman, L., Raaijmakers, J. A., Johnson, J. P., and van der Saag, P. T. 12-O-tetradecanoyl-phorbol-13-ace. J. Biol. Chem., *269:* 6185–6192, 1994.

11. Iademarco, M. F., McQuillan, J. J., Rosen, G. D., and Dean, D. C. Characterization of the promoter for vascular cell adhesion molecule-1 (VCAM-1). J. Biol. Chem., *267:* 16323–16329, 1992.

12. Novak, U., Cocks, B. G., and Hamilton, J. A. A labile repressor acts through the NFκB-like binding sites of the human urokinase gene. Nucleic Acids Res., *19:* 3389–3393, 1991.

13. Huang, S., Robinson, J. B., DeGuzman, A., Bucana, C. D., and Fidler, I. J.

Blockade of nuclear factor-κB signaling inhibits angiogenesis and tumorigenicity of human ovarian cancer cells by suppressing expression of vascular endothelial growth factor and interleukin 8. Cancer Res., *60:* 5334–5339, 2000.

14. Huang, S., Pettaway, C. A., Uehara, H., Bucana, C. D., and Fidler, I. J. Blockade of NF-κB activity in human prostate cancer cells is associated with suppression of angiogenesis, invasion, and metastasis. Oncogene, *20:* 4188–4197, 2001.

15. Sunwoo, J. B., Chen, Z., Dong, G., Yeh, N., Crowl, B. C., Sausville, E., Adams, J., Elliott, P., and Van Waes, C. Novel proteasome inhibitor PS-341 inhibits activation of nuclear factor-κB, cell survival, tumor growth, and angiogenesis in squamous cell carcinoma. Clin. Cancer Res., *7:* 1419–1428, 2001.

16. Kumar, A. P., Garcia, G. E., Orsborn, J., Levin, V. A., and Slaga, T. J. 2-Methoxyestradiol interferes with NF-κB transcriptional activity in primitive neuroectodermal brain tumors: implications for management. Carcinogenesis, *24:* 209–216, 2003.

17. Pan, Q., Kleer, C. G., van Golen, K. L., Irani, J., Bottema, K. M., Bias, C., De Carvalho, M., Mesri, E. A., Robins, D. M., Dick, R. D., Brewer, G. J., and Merajver, S. D. Copper deficiency induced by tetrathiomolybdate suppresses tumor growth and angiogenesis. Cancer Res., *62:* 4854–4859, 2002.

18. Cox, C., Teknos, T. N., Barrios, M., Brewer, G. J., Dick, R. D., and Merajver, S. D. The role of copper suppression as an antiangiogenic strategy in head and neck squamous cell carcinoma. Laryngoscope, *111:* 696–701, 2001.

19. van Golen, K. L., Bao, L. W., Brewer, G. J., Pienta, K. J., Kamradt, J. M., Livant, D. L., and Merajver, S. D. Suppression of tumor recurrence and metastasis by a combination of the PHSCN sequence and the antiangiogenic compound tetrathiomolybdate in prostate carcinoma. Neoplasia, *4:* 373–379, 2002.

20. Kleer, C. G., van Golen, K. L., and Merajver, S. D. Molecular biology of breast cancer metastasis. Inflammatory breast cancer: clinical syndrome and molecular determinants. Breast Cancer Res., *2:* 423–429, 2000.

21. van Golen, K. L., Wu, Z. F., Qiao, X. T., Bao, L. W., and Merajver, S. D. RhoC GTPase overexpression modulates induction of angiogenic factors in breast cells. Neoplasia, *2:* 418–425, 2000.

22. van Golen, K. L., Wu, Z. F., Qiao, X. T., Bao, L. W., and Merajver, S. D. RhoC GTPase, a novel transforming oncogene for human mammary epithelial cells that partially recapitulates the inflammatory breast cancer phenotype. Cancer Res., *60:* 5832–5838, 2000.

23. Pavlakovic, H., Havers, W., and Schweigerer, L. Multiple angiogenesis stimulators in a single malignancy: implications for anti-angiogenic tumor therapy. Angiogenesis, *4:* 259–262, 2001.

24. Redman, B. G., Esper, P., Dunn, R. L., Pan, Q., Merajver, S. D., Hussain, H. K., Chenevert, T., and Brewer, G. J. Phase II trial of tetrathiomolybdate in patients with advanced kidney cancer. Clin. Cancer Res., *9:* 1666–1672, 2003.